CASE REPORT

J Jpn Soc Intensive Care Med. 2010;17:179～184.

Analysis of cytokine/chemokine levels in bronchoalveolar lavage fluids from patients with acute respiratory distress syndrome

Yuka Osaki[*1], Yasuhiro Maehara[*1], Masaki Sato[*1], Akiyoshi Hoshino[*2], Kenji Yamamoto[*2], Tomokazu Nagao[*3], Kazuo Suzuki[*3], Shoji Kawachi[*1]

Abstract: Bronchoalveolar lavage (BAL) was performed in 5 patients with acute respiratory distress syndrome (ARDS; ARDS group hereafter) and 2 patients with respiratory failure (non-ARDS group hereafter) within 3 hours of intubation before ARDS treatment other than mechanical ventilation. ARDS was diagnosed based on the criteria defined by the American-European Consensus Conference. BAL fluid (BALF) and sera samples were obtained on the same occasion. The presence of 17 cytokines/chemokines in these specimens was simultaneously determined using a Bio-Plex® Suspension Array System. The levels of these cytokines/chemokines in BALF and sera samples were compared between the ARDS group and the non-ARDS group. The levels of chemokine granulocyte colony-stimulating factor (G-CSF), monocyte chemoattractant protein-1 (MCP-1) (monocyte chemoattractant factor), and macrophage inflammatory protein-1β (MIP-1β) in the BALF samples were significantly higher in the ARDS group than in the non-ARDS group. The level of pro-inflammatory cytokine interleukin (IL)-6 in BALF was also higher in the ARDS group than in the non-ARDS group. In contrast, the levels of IL-1β and IL-8 in BALF were higher in the non-ARDS group than in the ARDS group. The levels of these cytokines in BALF were higher than the corresponding sera levels in both groups. These results indicate that severe initial alveolar injury significantly activates chemokines in patients with ARDS caused by direct lung injury (such as pneumonia), unlike the increased levels of the inflammatory cytokines IL-1β and IL-8 in BALF of patients with early ARDS.

Key words: ①acute respiratory distress syndrome (ARDS), ②cytokines/chemokines, ③bronchoalveolar lavage (BAL)

Introduction

Acute respiratory distress syndrome (ARDS), which has various underlying etiologies, is a rapidly progressive disorder. The acute phase is characterized by the rapid onset of respiratory failure and arterial hypoxemia refractory to supplemental oxygen therapy. A new definition for ARDS was recommended by the American-European Consensus Conference Committee in 1994, enabling standardized clinical research and trials to become possible [1]. The clinical disorders thought to be responsible for ARDS can be categorized into two groups: direct pulmonary injury, such as pneumonia (pulmonary etiology); and indirect lung injury, such as sepsis (extra-pulmonary etiology) [1]. In the present study, we compared the cytokine levels of ARDS patients with pneumonia (no initial extra-pulmonary injury) and pneumonia patients without ARDS to clarify the factors responsible for the onset of ARDS.

The pathological findings of ARDS include diffuse alveolar damage and extravasation of the intravascular fluid. Inflammation was also identified as a key feature in the 1994 Consensus Conference on ARDS [1]. The formation of inflammatory mediators is now widely regarded to play an important role in the pathophysiology of inflammation in ARDS [2]. These mediators include tumor necrosis factor (TNF)-α and interleukin (IL)-1, IL-4, IL-6, IL-8, IL-10, and IL-13 [3]. C5a, the expression

This article is featured in "HIGHLIGHTS IN THIS ISSUE". Please see the issue of J Jpn Soc Intensive Care Med 2010; 17: 131-132.

[*1] Division of Anesthesiology, Surgical Operation Department,
[*2] International Clinical Research Center, International Medical Center of Japan
1-21-1 Toyama, Shinjuku-ku, Tokyo 162-8655, Japan
[*3] Inflammation Program, Department of Immunology, Chiba University Graduate School of Medicine
1-8-1 Inohana, Chuo-ku, Chiba, Chiba 260-8670, Japan

Submitted for publication January 29, 2009
Accepted for publication July 3, 2009

Table 1 Demographic characteristics

Patient No.	Gender	Age	Coexisting disease	Diagnosis	Cause of ARDS
1	F	37	Wegener's granulomatosis	ARDS	Pneumonia (*Candida*)
2	F	64	Rheumatoid arthritis	ARDS	Pneumonia (bacterial)
3	M	45	Drug-induced pneumonitis	Pneumonitis	—
4	M	47	Bacterial pneumonia	Pneumonia	—
5	M	59	Multiple myeloma	ARDS	Pneumonia (bacterial)
6	M	43	MDS, pneumonia	ARDS	Pneumonia (fungus)
7	F	45	Influenza type-A infection	ARDS	Pneumonia (bacterial)

ARDS, acute respiratory distress syndrome; F, female; M, male; MDS, myelodysplastic syndrome.

of which is considered to be a major contributor to the inflammatory pathway in sepsis [4),5)] but is not involved in the final common pathway to acute lung injury (ALI) / ARDS, is complemented by the expression of chemokines, cytokines, and lipid signaling molecules [2),3)]. On the other hand, the acute phase of ARDS is characterized by the influx of neutrophils as a consequence of the disruption of alveolar-capillary barrier [6)]. Activated alveolar macrophages secrete cytokines, which activate the inflammatory cascade and neutrophils; this in turn stimulates the infiltration of neutrophils [7)]. Although the levels of these cytokines/chemokines have been individually determined using enzyme-linked immunosorbent assay (ELISA) systems, the levels of inflammatory cytokines and chemokines must be simultaneously determined using a small sample to fully understand the involvements of inflammatory cytokines and chemokines in ARDS. Recently, the Bio-Plex® Suspension Array System (Bio-Rad Laboratories, Inc., USA) has been established for the simultaneous determination of cytokines/chemokines in small samples of 15–50 μl, enabling a comprehensive analysis [8)].

In the present study, bronchoalveolar lavage (BAL) was performed in patients with ARDS or acute respiratory failure who were receiving mechanical ventilation. The levels of 17 cytokines/chemokines in BAL fluid (BALF) were compared between patients with ARDS and those with moderate respiratory failure arising from other causes to clarify the roles of cytokines and chemokines as inflammatory mediators in patients with ARDS.

Materials and methods

Patients: This study was approved by the Ethics Committee of the International Medical Center of Japan (No. 449-H19). Written informed consent was obtained from all the patients.

Patients were diagnosed as having ARDS or ALI according to the definitions of the American-European Consensus Conference Committee [1)].

Mechanical ventilation: Mechanical ventilation was initiated in all the patients while they were in our hospital's ICU; all the patients had severe arterial hypoxemia that was refractory to supplemental oxygen treatment. The mechanical ventilation parameters in the ARDS patients were decided based on the *Lung Protective Strategy* of the American-European Consensus Conference Committee [9)].

BALF and sera samples: BAL was performed within 3 hours of the start of mechanical ventilation and before the start of specific treatment for ARDS other than mechanical ventilation. The BAL procedure was performed using a fiber-optic bronchoscope with 3 aliquots of 50 m*l* of warm sterile saline, infusing 50 m*l* of warm sterile saline into a segment of the lung and aspirating the fluid back into each aliquot (more than 50% recovery). The first aliquot was discarded, and the third aliquot was saved and used for the assays. Sera samples were also obtained from the patients on the same occasion.

Laboratory processing and assay: The BALF and sera samples intended for the cytokine/chemokine assay were immediately processed and then stored at −80℃.

The Bio-Plex® Suspension Array System was used for the cytokine/chemokine assay, enabling the levels of 17 cytokines/chemokines; interleukin (IL)-2, IL-4, IL-6, IL-8, IL-10, granulocyte macrophage colony stimulating factor (GM-CSF), interferon-γ (IFN-γ), TNF-α, IL-1β, IL-5, IL-7, IL-12 (P70), IL-13, IL-17, granulocyte colony-stimulating factor (G-CSF), monocyte chemoattractant protein-1 (MCP-1) (monocyte chemoattractant factor, MCAF), and macrophage inflammatory protein-1β (MIP-1β), to be measured simultaneously. The cytokines/chemokines were measured using the fluorescent microbeads method.

Results

Clinical data: Seven patients were enrolled in this study. Their demographic data are shown in Table 1; 5 patients were diagnosed as having ARDS (ARDS group; P/F ratio was grade 4 in 4 patients and grade 3 in 1 patient according to the Murray Lung Injury Score [10)]), and the remaining 2 patients were diagnosed as having acute respiratory failure (non-ARDS group; 1 patient was within the definition for ALI [200 < P/F ratio < 300]). Of the 7 patients, 6 survived and were discharged from the ICU and 1 died while in the ICU. In the ARDS patients, mechanical ventilation was initiated using the controlled mechanical ventilation (CMV) (continuous positive pressure ventilation (CPPV) mode), and the initial ventilator settings were as follows: tidal volume, 6 m$l \cdot kg^{-1}$;

Table 2 Characteristics of lung injuries and outcomes

Patient No.		1	2	3	4	5	6	7
Onset day		5	3	8	5	3	2	6
Vital signs (before tracheal intubation)	Body temperature (℃)	37.2	39.0	35.9	39.0	39.0	38.5	39.5
	Respiratory rate (min^{-1})	18	33	20	32	40	37	28
	Heart rate (min^{-1})	100	110	88	120	146	120	140
	Blood pressure (mmHg)	90/60	120/65	98/68	125/85	40/20	140/95	124/54
Initial mechanical ventilation setting (after tracheal intubation)	Tidal volume ($ml \cdot kg^{-1}$)	6	6	−	8	6	6	6
	PEEP (cmH_2O)	10	12	4	6	12	10	12
	F_IO_2	1.0	1.0	0.4	1.0	1.0	1.0	1.0
	Mode	CPPV	CPPV	Spontaneous	SIMV	CPPV	CPPV	CPPV
	Respiratory rate (min^{-1})	30	30	−	10	25	25	30
Bilateral infiltrations (chest X-ray)		+	+	+	−	+	+	+
Signs of CHF		−	−	−	−	−	−	−
P/F ratio		125	98	404	220	63	82	93
Diagnosis		ARDS	ARDS	Pneumonitis	Pneumonia	ARDS	ARDS	ARDS
Mortality		Alive	Alive	Alive	Alive	Alive	Dead	Alive

ARDS, acute respiratory distress syndrome; CHF, congestive heart failure; CPPV, continuous positive pressure ventilation; SIMV, synchronized intermittent mandatory ventilation.

respiratory rate, 25–30 · min^{-1}; PEEP (positive end-expiratory pressure), 10–12 cmH_2O; peak inspiratory pressure, below 30 cmH_2O; F_IO_2, 1.0 (Table 2).

Cytokine and chemokine levels in BALF —ARDS and non-ARDS groups (Fig. 1): The levels of G-CSF (8,504 vs. 106 pg · ml^{-1}, mean values), MCP-1 (MCAF) (3,024 vs. 59 pg · ml^{-1}) and MIP-1β (1,181 vs. 126 pg · ml^{-1}) in the BALF were higher in the ARDS group than in the non-ARDS group. The level of IL-6 was also elevated in the ARDS group, compared with that in the non-ARDS group (919 vs. 34 pg · ml^{-1}). On the other hand, the levels of IL-1β (51 vs. 501 pg · ml^{-1}) and IL-8 (761 vs. 2,247 pg · ml^{-1}) were higher in the non-ARDS group than in the ARDS group.

Cytokine and chemokine levels in sera —ARDS and non-ARDS groups (Fig. 2): The serum levels of IL-7 (32 vs. 0 pg · ml^{-1}, mean values), IL-13 (21 vs. 4 pg · ml^{-1}), GM-CSF (128 vs. 52 pg · ml^{-1}) and G-CSF (364 vs. 86 pg · ml^{-1}) were higher in the ARDS group than in the non-ARDS group. However, the serum levels of TNF-α (15 vs. 94 pg · ml^{-1}), IFN-γ (168 vs. 338 pg · ml^{-1}), IL-6 (317 vs. 402 pg · ml^{-1}) and MIP-1β (40 vs. 311 pg · ml^{-1}) were higher in the non-ARDS group than in the ARDS group.

Discussion

ARDS is characterized by the acute onset of diffuse and severe inflammation [7]. The underlying causes have been classified into those causing direct lung injury and those causing indirect lung injury. Although some recent strategies and trials have been successful and have contributed to a decline in the mortality rate, the mortality rate of ARDS remains high [11)~13)]. The outcome of ARDS is considered to depend on the degree of alveolar epithelial injury. Clinical and experimental studies have demonstrated the evidence of neutrophil-mediated lung injury in ARDS and ALI [14)]. Neutrophils are recognized as major contributors in the pathogenesis of ARDS [2)], and a complex network of inflammatory cytokines plays an important role in the development of ARDS [2),3)].

One of the characteristic findings of this study was the remarkably elevated BALF levels of G-CSF, MCP-1 (MCAF) and MIP-1β, which are all chemokines, in the ARDS group, compared with those in the non-ARDS group. These findings differ from those of previous reports, in which TNF-α and IL-1β were described as being elevated in BALF and sera of patients with ARDS [15)~17)].

TNF-α and IL-1β are thought to be produced by activated macrophages during the acute phase of ARDS, leading to the induction.of IL-6 and IL-8 and the subsequent activation of a network of cytokines [14),16),17)]. Once the inflammatory cascade has been activated by this cytokine network, neutrophils migrate into the alveolar space [17)]. Thus, in cases of ARDS with direct lung injury, the excessive activation of chemokines is thought to occur. The production of excess amounts of chemokines

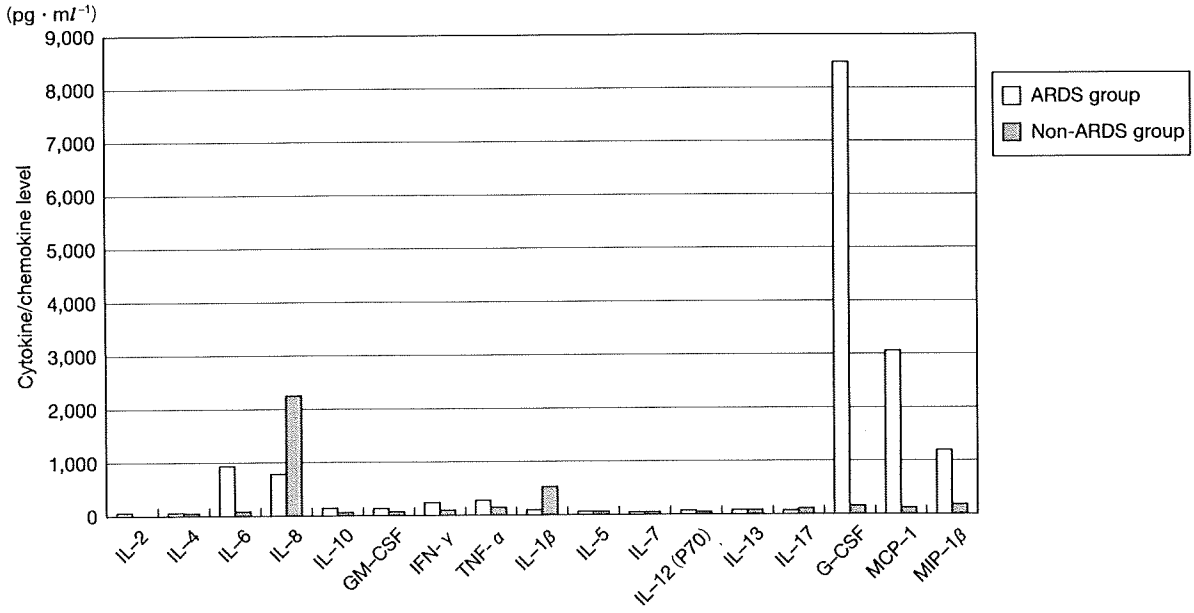

Fig. 1 Cytokine/chemokine levels in BALF
G-CSF, granulocyte colony-stimulating factor; GM-CSF, granulocyte macrophage colony stimulating factor; IFN-γ, interferon-γ; IL, interleukin; TNF, tumor necrosis factor; MCP-1, monocyte chemoattractant protein-1; MIP-1β, macrophage inflammatory protein-1β.

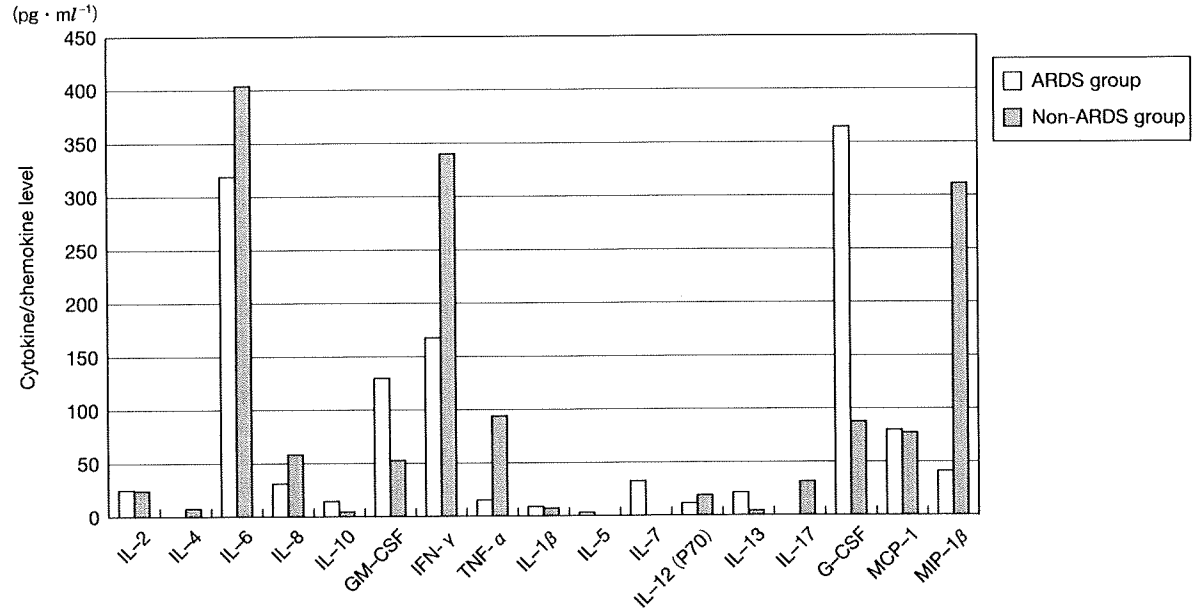

Fig. 2 Cytokine/chemokine levels in sera
G-CSF, granulocyte colony-stimulating factor; GM-CSF, granulocyte macrophage colony stimulating factor; IFN-γ, interferon-γ; IL, interleukin; TNF, tumor necrosis factor; MCP-1, monocyte chemoattractant protein-1; MIP-1β, macrophage inflammatory protein-1β.

in the alveolar region is, in turn, thought to enhance the infiltration of neutrophils, resulting in the induction of direct damage to the lung.

Two possibilities might explain the extraordinarily high levels of chemokines in the BALF samples from the ARDS group in the present study. One is the different time-points at which the BALF specimens were obtained, and the other is the difference in the types of disorders that were associated with ARDS and acute respiratory failure in the study groups. In the present study, ARDS was associated with direct lung injury in all 5 cases. We performed BAL within 3 hours of the initiation of

mechanical ventilation in each patient; among the studies reported to date, this is the earliest reported time-point at which BALF specimens were obtained [14)~16)]. In most previous studies, the BALF specimens were obtained within 24 hours. Thus, the BALF findings in the present study may not have been affected by ventilation-induced lung injury or ongoing inflammation. The levels of cytokines in BALF and sera might change drastically over the first 24 hours after intubation.

Rosseau et al. [18)] suggested that a significant correlation existed between the BALF MCP-1 concentration (reflecting a predominance of monocyte-like alveolar macrophages) and the severity of respiratory failure. In ARDS caused by direct lung injury, activated macrophages, monocytes and neutrophils cause inflammation of the lung, resulting in an increased production of GCSF, MCP-1 and MIP-1β. Lung injury in cases with ARDS is more severe than that in cases without ARDS and is associated with high levels of G-CSF, MCP-1 and MIP-1β.

Another reason for the high levels of chemokines seen in our study may be the difference in the spectra of diseases associated with ARDS, since all the ARDS patients in the present study had direct lung injury. Elevations in cytokine/chemokine levels are thought to depend on whether the injury to the lung is direct or indirect. In ARDS associated with direct lung injury, the inflammation is thought to be more severe and to be associated with higher levels of cytokines/chemokines than that in ARDS associated with indirect lung injury.

Similar results to ours have been demonstrated in one previous study. Nakano et al. [19)] measured the levels of cytokines in 4 cases with ARDS and 8 normal controls and reported significantly higher levels of 16 cytokines/chemokines in the BALF specimens from the ARDS patients. Although the report did not describe the specific time-point at which the BALF specimens were obtained, the authors suggested that cytokine and chemokine influx from the plasma into the alveoli may be responsible for the excessive elevations of the cytokine/chemokine levels in BALF. According to our study, however, the cytokine/chemokine levels in BALF were higher than the cytokine levels in sera during the early phase of ARDS and were not the result of cytokine/chemokine influx from the plasma.

Among chemokines, IL-8 has one of the strongest effects on neutrophils. Although a previous report concluded that IL-8 was a reliable predictor of the development of ARDS [20)], our results suggest that this is not necessarily true. In our study, the levels of IL-1β and IL-8 in BALF were higher in the non-ARDS group than in the ARDS group. Because IL-8 is a chemotactic factor for neutrophils, the induction of IL-8 has already occurred once bacterial infection is observed in the lung (as in pneumonia). Thus, the levels of these cytokines are elevated not only in cases with ARDS, but also in cases with a high risk of ARDS, and elevated IL-8 levels might reflect the overall clinical severity, rather than pulmonary injury in ARDS [21)]. The systemic levels of TNF-α and IL-1β have also been reported to reflect the severity of lung injury and not to have any diagnostic value [15)].

Sivelestat is known as a reversible, competitive inhibitor of neutrophil elastase. Although its efficacy remains controversial, it has been shown to be effective in animal models and has been demonstrated to have beneficial effects on pulmonary function [22)]. However, the Sivelestat Trial in ALI Patients Requiring Mechanical Ventilation (STRIVE) study [23)] has demonstrated that the intravenous administration of a neutrophil elastase inhibitor had no effect on the 28-day all-cause mortality rate or the number of ventilator-free days in a heterogeneous group of patients with acute lung injury. Considering the pathogenesis of ARDS, neutrophil elastase inhibitors might be effective if they were used in cases of ARDS caused by direct lung injury.

Two possible limitations of this study should be mentioned: the number of cases was quite small, and ARDS was caused by direct lung injury in all of the reported cases. Further investigations using a larger number and a wider spectrum of ARDS patients, including cases caused by direct and indirect lung injury, are warranted.

Acknowledgements

This study was supported by Health and Labour Sciences Research Grants (H19-Sinko-Ippan-005). The substance of this paper was presented at the 35th Annual Meeting of the Japanese Society of Intensive Care Medicine in Tokyo, in February 2008.

References

1) Bernard GR, Artigas A, Brigham KL, et al. The American-European Consensus Conference on ARDS. Definitions, mechanisms, relevant outcomes, and clinical trial coordination. Am J Respir Crit Care Med. 1994;149:818-24.
2) Matthay MA, Zimmerman GA. Acute lung injury and the acute respiratory distress syndrome: four decades of inquiry into pathogenesis and rational management. Am J Respir Cell Mol Biol. 2005;33:319-27.
3) Park WY, Goodman RB, Steinberg KP, et al. Cytokine balance in the lungs of patients with acute respiratory distress syndrome. Am J Respir Crit Care Med. 2001;164:1896-903.
4) Riedemann NC, Guo RF, Neff TA, et al. Increased C5a receptor expression in sepsis. J Clin Invest. 2002;110:101-8.
5) Gerard C. Complement C5a in the sepsis syndrome--too much of a good thing? N Engl J Med. 2003;348:167-9.
6) Ware LB, Matthay MA. The acute respiratory distress syndrome. N Engl J Med. 2000;342:1334-49.
7) Puneet P, Moochhala S, Bhatia M. Chemokines in acute respiratory distress syndrome. Am J Physiol Lung Cell Mol Physiol. 2005;288:L3-15.
8) Hoshino A, Nagao T, Nagi-Miura N, et al. MPO-ANCA induces IL-17 production by activated neutrophils *in vitro* via classical complement pathway-dependent manner. J Autoimmun. 2008;31:79-89.
9) Artigas A, Bernard GR, Carlet J, et al. The American-European Consensus Conference on ARDS, part 2. Ventilatory, pharmacologic, supportive therapy, study design strategies, and issues related to recovery and remodeling. Am J Respir Crit Care Med. 1998;157:1332-47.

10) Murray JF, Matthay MA, Luce JM, et al. An expanded definition of the adult respiratory distress syndrome. Am Rev Respir Dis. 1988;138:720-3.
11) The Acute Respiratory Distress Syndrome Network. Ventilation with lower tidal volumes as compared with traditional tidal volumes for acute lung injury and the acute respiratory distress syndrome. N Engl J Med. 2000;342:1301-8.
12) Steinberg KP, Hudson LD, Goodman RB, et al. National Heart, Lung, and Blood Institute Acute Respiratory Distress Syndrome (ARDS) Clinical Trials Network. Efficacy and safety of corticosteroids for persistent acute respiratory distress syndrome. N Engl J Med. 2006;354:1671-84.
13) McIntyre RC Jr, Pulido EJ, Bensard DD, et al. Thirty years of clinical trials in acute respiratory distress syndrome. Crit Care Med. 2000;28:3314-31.
14) Matute-Bello G, Liles WC, Radella F 2nd, et al. Neutrophil apoptosis in the acute respiratory distress syndrome. Am J Respir Crit Care Med. 1997;156:1969-77.
15) Millar AB, Foley NM, Singer M, et al. Tumour necrosis factor in bronchopulmonary secretions of patients with adult respiratory distress syndrome. Lancet. 1989;2:712-4.
16) Meduri GU, Kohler G, Headley S, et al. Inflammatory cytokines in the BAL of patients with ARDS. Persistent elevation over time predicts poor outcome. Chest. 1995;108:1303-14.
17) Bauer TT, Montón C, Torres A, et al. Comparison of systemic cytokine levels in patients with acute respiratory distress syndrome, severe pneumonia, and controls. Thorax. 2000; 55:46-52.
18) Rosseau S, Hammerl P, Maus U, et al. Phenotypic characterization of alveolar monocyte recruitment in acute respiratory distress syndrome. Am J Physiol Lung Cell Mol Physiol. 2000; 279:L25-35.
19) Nakano Y, Fujishima S, Miyasho T, et al. Simultaneous measurement of multiple cytokines by a bead array method in bronchoalveolar lavage fluid of patients with ALI/ARDS. Jpn J Resp Care. 2007;24:140-5.
20) Jorens PG, Van Damme J, De Backer W, et al. Interleukin 8 (IL-8) in the bronchoalveolar lavage fluid from patients with the adult respiratory distress syndrome (ARDS) and patients at risk for ARDS. Cytokine. 1992;4:592-7.
21) Chollet-Martin S, Montravers P, Elbim C, et al. High levels of interleukin-8 in the blood and alveolar spaces of patients with pneumonia and adult respiratory distress syndrome. Infect Immun. 1993;61:4553-9.
22) Okayama N, Kakihana Y, Setoguchi D, et al. Clinical effects of a neutrophil elastase inhibitor, sivelestat, in patients with acute respiratory distress syndrome. J Anesth. 2006;20:6-10.
23) Zeiher BG, Artigas A, Vincent JL, et al. Neutrophil elastase inhibition in acute lung injury: results of the STRIVE study. Crit Care Med. 2004;32:1695-702.

Serial Review J. Clin. Biochem. Nutr., 46, 14–19, January 2010

Heme Oxygenase and Carbon Monoxide: Medicine Chemistry and Biological Effects
Guest Editor: Yuji Naito

A New Paradigm for Antimicrobial Host Defense Mediated by a Nitrated Cyclic Nucleotide

Tatsuya Okamoto, Shahzada Khan, Kohta Oyama, Shigemoto Fujii, Tomohiro Sawa and Takaaki Akaike*

Department of Microbiology, Graduate School of Medical Sciences, Kumamoto University, Kumamoto 860-8556, Japan

Received 13 July, 2009; Accepted 18 September, 2009

Summary **Nitric oxide (NO), produced by inducible NO synthase (iNOS) during infection, plays a crucial role in host defense mechanisms. *Salmonella typhimurium* infection in mice is associated with excessive production of NO from iNOS as a host defense response. An important cytoprotective and antimicrobial function of NO is mediated by induction of heme oxygenase (HO)-1. The signaling mechanism of NO-dependent HO-1 induction has remained unclear, however. We recently discovered a nitrated cyclic nucleotide, 8-nitroguanosine 3',5'-cyclic monophosphate (8-nitro-cGMP), which is formed via guanine nitration with NO and reactive oxygen species. iNOS-dependent 8-nitro-cGMP formation and HO-1 induction were identified in *Salmonella*-infected mice. Extensive apoptosis observed with iNOS-deficient macrophages infected with *Salmonella* was remarkably suppressed via HO-1 induced by 8-nitro-cGMP formed in cells. This cytoprotective signaling appears to be mediated by the reaction of 8-nitro-cGMP with protein sulfhydryls to generate a novel post-translational modification named protein *S*-guanylation. We also found that 8-nitro-cGMP specifically *S*-guanylates Keap1, a negative regulator of transcription factor Nrf2, which in turn up-regulates transcription of HO-1. Here, we discuss the unique mechanism of NO-mediated host defense that operates via formation of a novel signaling molecule - 8-nitro-cGMP - during microbial infections.**

Key Words: **nitric oxide, host defense, 8-nitro-cGMP, heme oxygenase-1, protein *S*-guanylation**

Introduction

Nitric oxide (NO) plays a crucial role in innate host defense mechanisms against microbial infection. Regardless of the type of pathogen, whether bacteria, viruses, or fungi, an inducible NO synthase (iNOS) is induced almost universally during the infection process. This induction occurs in various cells after recognition by host cells of microbial structural components (e.g., lipopolysaccharides, lipoteichoic acid, peptidoglycans, and fungal polysaccharides) and nucleic acid components (such as dsRNA, ssRNA, and CpG DNA) via pattern recognition receptors including Toll-like receptors [*1*]. iNOS induction is synergistically enhanced by inflammatory cytokines and interferon produced during infection [*2*]. NO produced by iNOS reportedly reacts with simultaneously generated reactive oxygen species (ROS), is converted to reactive nitrogen species (RNS), such as per-

*To whom correspondence should be addressed.
Tel: +81-96-373-5100 Fax: +81-96-362-8362
E-mail: takakaik@gpo.kumamoto-u.ac.jp

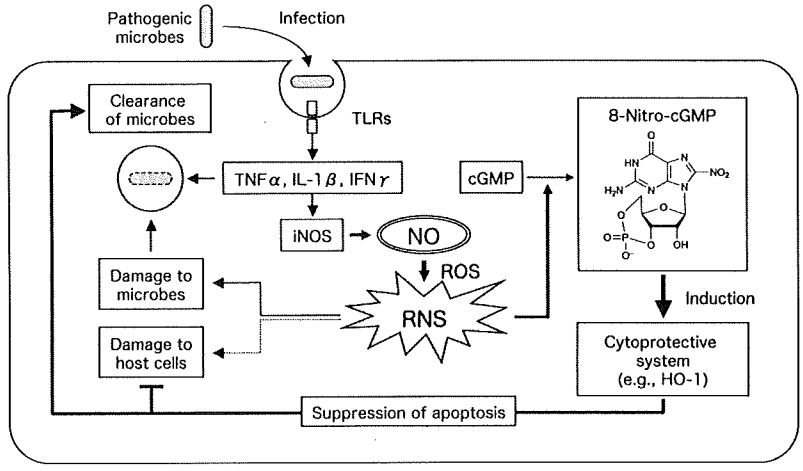

Fig. 1. iNOS induction and NO-mediated host defense mechanism against microbial infection. NO overproduced by iNOS induced during microbial infection is converted to reactive nitrogen species (RNS) via reaction with reactive oxygen species (ROS). RNS have two opposite biological effects: potent bactericidal activity contributing to host defense and damage of cells and tissues of the host. 8-Nitro-cGMP may function as a signaling molecule mediating oxidative stress responses, such as HO-1 induction, and it may play a crucial role in the innate host immunity.

oxynitrite ($ONOO^-$) and nitrogen dioxide (NO_2), and may demonstrate direct antimicrobial activities (Fig. 1) [*3–5*]. In fact, infection with *Salmonella typhimurium*, a facultative intracellular bacterium, causes excessive production of NO via iNOS induction, along with microabscess formation, in the liver in mice. A comparative experiment with iNOS-deficient ($iNOS^{-/-}$) and wild-type mice demonstrated that the bacterial growth in the liver and mortality in $iNOS^{-/-}$ mice were significantly higher than those in wild-type mice. This finding indicates that NO from iNOS participates in host defense against infection, possibly by means of antimicrobial activity [*3*].

In contrast, NO and ROS also reportedly damage host cells and tissues, which causes oxidative stress. In a murine influenza virus-infected pneumonia model, iNOS expression increased in infected lungs, especially in the respiratory epithelium and alveolar macrophages, with resultant excessive production of NO [*6, 7*]. However, unlike progression of *Salmonella* infection, progression of pneumonia is well correlated with iNOS induction; pneumonia was less severe and mortality was lower in $iNOS^{-/-}$ mice than in wild-type mice [*6, 8*]. In general, NO and ROS show antibacterial activity, but because they have no effective antiviral activity, they cause nonspecific damage of host cells and tissues. Therefore, the role of NO in the pathogenesis of infection is known as a double-edged sword (Fig. 1) [*6, 8*].

Recently, much attention has focused on the signaling functions of NO and ROS. NO can suppress apoptosis of host cells caused by infection, and it is involved, together with ROS, in responses to oxidative stress [*9–11*] (Fig. 1). Here, we reexamine the role of NO and ROS in host defense against infection, with a focus on a unique signaling function of the nitrated cyclic nucleotide 8-nitroguanosine 3',5'-cyclic monophosphate (8-nitro-cGMP), which mediates cytoprotective oxidative stress responses occurring during infections.

NO- and ROS-dependent Formation of 8-Nitro-cGMP

NO was initially discovered as a signaling molecule regulating vascular tone and neuronal systems [*12, 13*]. These functions are mainly mediated through a guanosine 3',5'-cyclic monophosphate (cGMP)-dependent mechanism, but other pathways that are not directly related to cGMP appear to be responsible for many aspects of NO signaling [*14–16*]. Although NO has diverse pathophysiological functions, NO itself is an inert molecule. Much of its chemical reactivity depends on RNS generated through the reaction with ROS produced together with in various cells. The reaction of NO with O_2 and superoxide (O_2^-), and the reaction of nitrite (NO_2^-) with the H_2O_2-peroxidase system lead to the generation of RNS [*17–19*]. NO- and ROS-derived RNS have strong nitration potentials for various biological molecules such as proteins, lipids, and nucleic acids, and they possess cGMP-independent signaling functions, as mentioned above.

In fact, nitrated guanine derivatives, such as 8-nitroguanine and 8-nitroguanosine, are known to be formed by RNS, and their formation was identified in various cultured cells and in tissues from influenza virus-infected mice with viral pneumonia and humans with lung disease [*8, 20, 21*]. We recently clarified the NO- and ROS-dependent formation of

a nitrated cyclic nucleotide, 8-nitro-cGMP, as a completely new derivative of cGMP (Fig. 1) [*22*]. *In vitro* experiments showed that reaction of cGMP with authentic peroxynitrite and with the nitrite/H_2O_2-peroxidase system generated 8-nitro-cGMP, but NO alone did not, which indicates that RNS are involved in nitration of cGMP (unpublished observation). We developed an anti-8-nitro-cGMP monoclonal antibody and immunostained cytokine-stimulated macrophage-like cells (RAW264.7 cells) to demonstrate that 8-nitro-cGMP formation depended on production of both NO and ROS [*22*]. Moreover, *Salmonella* infection in cultured murine macrophages generated 8-nitro-cGMP in wild-type mice but not in iNOS$^{-/-}$ mice. Furthermore, immunostaining analysis of liver tissue from *Salmonella*-infected mice demonstrated abundant 8-nitro-cGMP generation in wild-type mice but not in iNOS$^{-/-}$ mice [*23*]. This NO-dependent 8-nitro-cGMP formation was also observed in lung tissue from influenza virus-infected mice (unpublished data), which indicated that 8-nitro-cGMP was produced in an iNOS-dependent manner *in vivo*.

NO-mediated Induction of the Cytoprotective Molecule HO-1

During infection, various cytoprotective and antioxidant systems are induced to protect cells and tissues from pathogenic microbes [*24–26*]. Heme oxygenase (HO)-1 is known as a factor that is rapidly induced during infection and that contributes to the host defense mechanism [*27*]. HO-1 degrades free heme, used as a substrate, into biliverdin, iron ions, and carbon monoxide (CO). Both biliverdin and iron ions carry out antioxidant activity by means of reduction to bilirubin and production of ferritin, respectively [*28*, *29*]. CO is known to exhibit cytoprotection via suppressing production of inflammatory cytokines and apoptosis [*30*]. HO-1 is reportedly induced by various stresses and by multiple transcription factors, e.g., heat shock factor 1 (HSF1), nuclear factor-κB (NF-κB), activator protein-1 (AP-1), and nuclear factor-erythroid 2-related factor 2 (Nrf2) (Fig. 2) [*27*]. Modulators that upregulate these transcription factors include heat shock or intracellular accumulation of abnormal proteins (HSF1), infection or inflammatory responses (NF-κB), abnormal cell growth (AP-1), and electrophiles or oxidants (Nrf2).

Analyses of HO-1 levels in *Salmonella*-infected mice demonstrated that both the amount of HO-1 protein and activity of HO-1 (as evidenced by blood CO levels) as well as its mRNA levels increased during infection, with induction seen mainly in macrophages [*23*]. Pharmacological inhibition of HO-1 activity increased bacterial growth (by approximately 10-fold) and apoptosis in liver tissues [*23*]. Therefore, HO-1 was suggested to function in host defense by suppressing macrophage apoptosis essential for elimination of *Salmonella* (Fig. 1). An important finding was lower levels of protein, mRNA, and activity of HO-1 in iNOS$^{-/-}$ mice compared with wild-type mice, which suggests the possible involvement of NO in HO-1 induction [*3*, *23*]. NO- and ROS-mediated induction of HO-1 has been reported from other groups [*10*, *31*].

The Unique Signaling Function of 8-Nitro-cGMP via Protein *S*-Guanylation

To further clarify the mechanisms of NO-mediated induction of HO-1, we used cultured macrophages from iNOS$^{-/-}$ mice to analyze the effect of authentic 8-nitro-cGMP. Treatment of iNOS$^{-/-}$ macrophages with 8-nitro-cGMP resulted in increased HO-1 levels in a manner that depended on time and concentration of 8-nitro-cGMP. In addition, HO-1 levels in *Salmonella*-infected macrophages were lower in iNOS$^{-/-}$ cells than in wild-type cells, but addition of 8-nitro-cGMP restored these lower levels to values comparable to those found in wild-type macrophages. Moreover, 8-nitro-cGMP treatment also markedly suppressed apoptosis associated with infection [*23*]. These findings suggest the possible involvement of 8-nitro-cGMP that is generated during infection in the signaling pathway of HO-1 induction (Fig. 1).

We further analyzed the molecular mechanisms governing 8-nitro-cGMP signaling functions. Because of its electrophilicity, 8-nitro-cGMP adducted with a sulfhydryl group of proteins via nucleophilic substitution with the nitro moiety of 8-nitro-cGMP to form a protein-*S*-cGMP adduct, which is a novel post-translational modification called protein *S*-guanylation (Fig. 2A) [*22*]. This protein adduct formation accompanies the denitration of 8-nitro-cGMP, with release of nitrite. Because 8-nitro-cGMP loses electrophilicity after S-guanylation, this electrophilic modification seems to be irreversible, at least under physiological conditions without specific catalysts yet to be identified. We found that one of the most important target proteins for *S*-guanylation is Kelch-like ECH-associated protein 1 (Keap1), which is now increasingly recognized as a potent redox-sensing protein. Keap1 is a negative regulator of Nrf2, which is a transcription factor regulating antioxidant enzymes for electrophiles and ROS [*32*, *33*]. Binding of Keap1 to Nrf2 inhibits Nrf2 transcriptional activity via sustaining rapid degradation of Nrf2 by proteasomes in the cytosolic compartment of cells. Keap1 is proposed to be a sensor protein for oxidative stress (Fig. 2B). Because Keap1 has highly reactive Cys residues, chemical modification of the Cys residue sulfhydryl groups by electrophiles and ROS is considered to trigger dissociation of Nrf2. Activated Nrf2 then translocates to nuclei to induce expression of various antioxidant and cytoprotective enzymes including HO-1, which contributes to the adaptive response to oxidative stress [*34–36*].

We thus examined whether Keap1 can indeed be modified

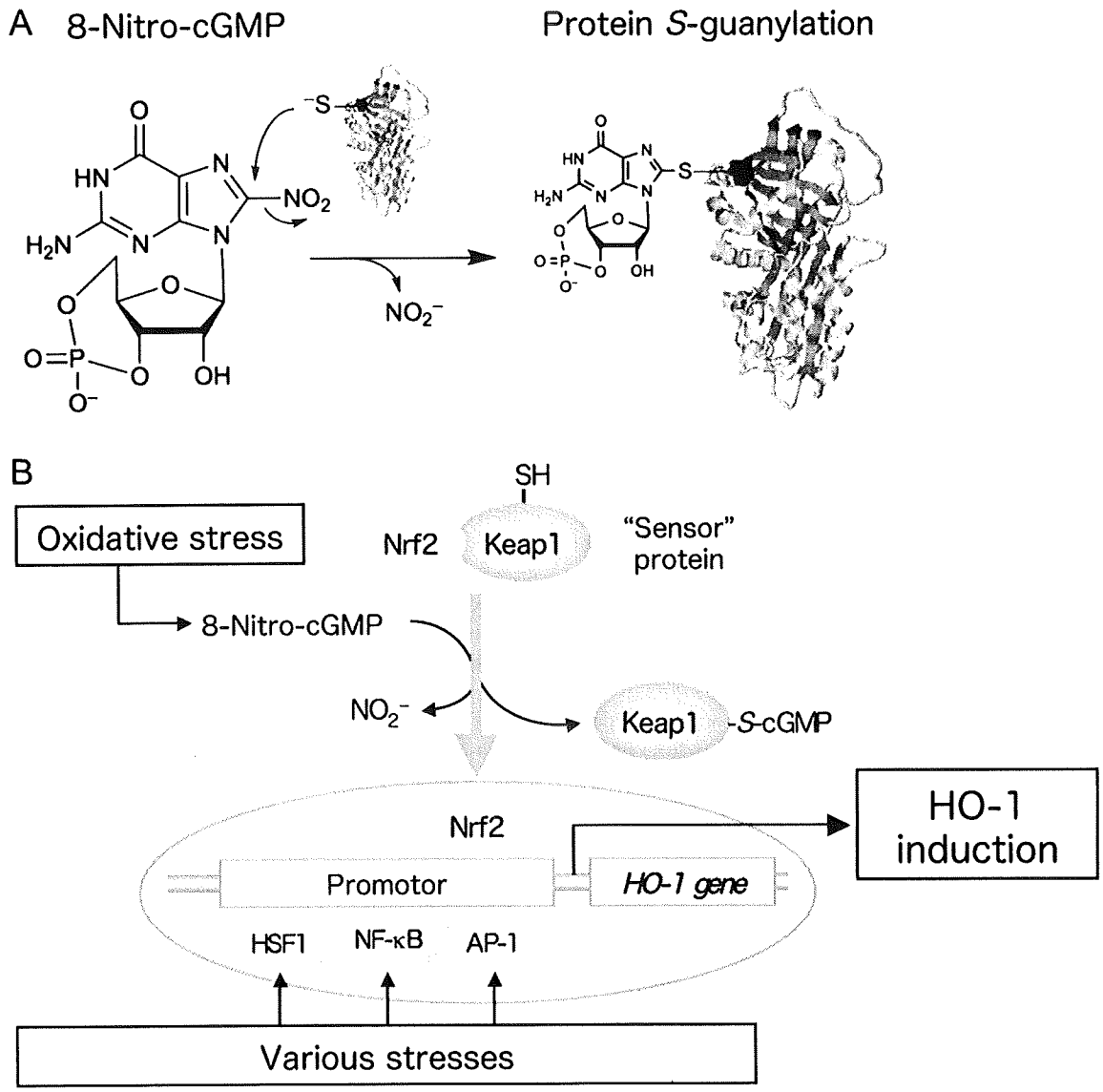

Fig. 2. New post-translational modification of proteins and HO-1 induction by 8-nitro-cGMP. (A) 8-Nitro-cGMP, a novel nitrated cyclic nucleotide generated from NO and ROS in cells, possesses an electrophilic property and causes *S*-guanylation of proteins, i.e., adduction of cGMP to protein sulfhydryls. (B) 8-Nitro-cGMP activates the Nrf2 pathway via S-guanylation of a sensor protein, Keap1, which leads to HO-1 induction.

by 8-nitro-cGMP produced via NO in cells. We infected cultured murine macrophages with *Salmonella*, and we found clear evidence of Keap1 *S*-guanylation by means of Western blotting using anti-*S*-guanylation antibody after isolation by immunoprecipitation [*22*, *23*]. We interpret these results to mean that 8-nitro-cGMP is involved in the major NO signaling pathway for cytoprotection and adaptive responses to ROS and oxidative stress through *S*-guanylation of Keap1. Strong support for this interpretation comes from the finding that cytoprotection and host defense conferred by 8-nitro-cGMP were clearly associated with increased HO-1 expression during *Salmonella* infection in macrophages and *in vivo*, as mentioned above [*23*] (Fig. 2B).

Beneficial and Pathological Effects of HO-1 in Various Microbial Infections

Analysis of the *Salmonella* infection model demonstrated that the NO-dependent and 8-nitro-cGMP-mediated signal pathway leads to HO-1 expression, and suppression of

apoptosis of infected macrophages potentiates microbial clearance—a host defense function against infection. However, some types of intracellular pathogens survive and multiply in macrophages because they escape the macrophage bactericidal system. One possible survival mechanism of these bacteria is, however, suppression of apoptosis of infected macrophages [*37*]. That is to say, HO-1 overexpression and resultant suppression of apoptosis are presumed to provide pathogens with a favorable intracellular environment so that they survive and grow. Similarly, inhibition of virus elimination by suppression of apoptosis of infected respiratory epithelial cells has been suggested as a potential pathogenic mechanism for the harmful effects of NO observed in a murine influenza virus-infected pneumonia model [*6*, *8*]. Although HO-1 induction via 8-nitro-cGMP is believed to contribute to host defense against infection [*23*, *38*, *39*], at the same time it may promote survival of particular pathogens (typically viruses). Various factors, such as the type of cells infected and the timing of HO-1 expression during infections, may lead to completely opposite biological effects of HO-1.

Conclusions

In summary, we have here clarified NO-dependent formation and cell signaling functions of 8-nitro-cGMP, which lead to expression of HO-1 and consequent cytoprotection in infected hosts. The 8-nitro-cGMP-mediated signaling pathway may protect host cells from apoptosis and support the antimicrobial effects of macrophages that are critically involved in innate immunity. Now in progress in our laboratory are further investigations of the antimicrobial functions of NO and 8-nitro-cGMP, with a special focus on potential target proteins of *S*-guanylation that is mediated by 8-nitro-cGMP, which may help establish a new understanding of host defense and microbial pathogenesis.

Acknowledgments

We thank Judith B. Gandy for her excellent editing of the manuscript. This work was supported in part by Grants-in-Aid for Scientific Research (B and C) and Grants-in-Aid for Scientific Research on Innovative Areas (Research in a Proposed Area) from the Ministry of Education, Culture, Sports, Science and Technology (MEXT) and Grants-in-Aid from the Ministry of Health, Labor and Welfare of Japan.

Abbreviations

8-nitro-cGMP, 8-nitroguanosine 3',5'-cyclic monophosphate; AP-1, activator protein-1; cGMP, guanosine 3',5'-cyclic monophosphate; HSF1, heat shock factor 1; HO, heme oxygenase; iNOS, inducible nitric oxide synthase; $iNOS^{-/-}$, iNOS-deficient; Keap1, Kelch-like ECH-associated protein 1; Nrf2, nuclear factor-erythroid 2-related factor 2; NF-κB, nuclear factor-κB; RNS, reactive nitrogen species; ROS, reactive oxygen species.

References

[1] Akira, S. and Takeda, K.: Toll-like receptor signalling. *Nat. Rev. Immunol.*, **4**, 499–511, 2004.

[2] Saura, M., Zaragoza, C., Bao, C., McMillan, A., and Lowenstein, C.J.: Interaction of interferon regulatory factor-1 and nuclear factor κB during activation of inducible nitric oxide synthase transcription. *J. Mol. Biol.*, **289**, 459–471, 1999.

[3] Alam, M.S., Akaike, T., Okamoto, S., Kubota, T., Yoshitake, J., Sawa, T., Miyamoto, Y., Tamura, F., and Maeda, H.: Role of nitric oxide in host defense in murine salmonellosis as a function of its antibacterial and antiapoptotic activities. *Infect. Immun.*, **70**, 3130–3142, 2002.

[4] Doi, T., Ando, M., Akaike, T., Suga, M., Sato, K., and Maeda, H.: Resistance to nitric oxide in *Mycobacterium avium* complex and its implication in pathogenesis. *Infect. Immun.*, **61**, 1980–1989, 1993.

[5] Umezawa, K., Akaike, T., Fujii, S., Suga, M., Setoguchi, K., Ozawa, A., and Maeda, H.: Induction of nitric oxide synthesis and xanthine oxidase and their roles in the antimicrobial mechanism against *Salmonella typhimurium* infection in mice. *Infect. Immun.*, **65**, 2932–2940, 1997.

[6] Akaike, T., Noguchi, Y., Ijiri, S., Setoguchi, K., Suga, M., Zheng, Y.M., Dietzschold, B., and Maeda, H.: Pathogenesis of influenza virus-induced pneumonia: involvement of both nitric oxide and oxygen radicals. *Proc. Natl. Acad. Sci. U.S.A.*, **93**, 2448–2453, 1996.

[7] Karupiah, G., Chen, J.H., Mahalingam, S., Nathan, C.F., and MacMicking, J.D.: Rapid interferon γ-dependent clearance of influenza A virus and protection from consolidating pneumonitis in nitric oxide synthase 2-deficient mice. *J. Exp. Med.*, **188**, 1541–1546, 1998.

[8] Akaike, T., Okamoto, S., Sawa, T., Yoshitake, J., Tamura, F., Ichimori, K., Miyazaki, K., Sasamoto, K., and Maeda, H.: 8-Nitroguanosine formation in viral pneumonia and its implication for pathogenesis. *Proc. Natl. Acad. Sci. U.S.A.*, **100**, 685–690, 2003.

[9] Brune, B., von Knethen, A., and Sandau, K.B.: Nitric oxide and its role in apoptosis. *Eur. J. Pharmacol.*, **351**, 261–272, 1998.

[10] Sandau, K., Pfeilschifter, J., and Brune, B.: Nitrosative and oxidative stress induced heme oxygenase-1 accumulation in rat mesangial cells. *Eur. J. Pharmacol.*, **342**, 77–84, 1998.

[11] Kim, Y.M., Bergonia, H., and Lancaster, J.R. Jr.: Nitrogen oxide-induced autoprotection in isolated rat hepatocytes. *FEBS Lett.*, **374**, 228–232, 1995.

[12] Bredt, D.S., Hwang, P.M., and Snyder, S.H.: Localization of nitric oxide synthase indicating a neural role for nitric oxide. *Nature*, **347**, 768–770, 1990.

[13] Murad, F.: Cyclic guanosine monophosphate as a mediator of

vasodilation. *J. Clin. Invest.*, **78**, 1–5, 1986.
[14] Martinez-Ruiz, A. and Lamas, S.: Two decades of new concepts in nitric oxide signaling: from the discovery of a gas messenger to the mediation of nonenzymatic posttranslational modifications. *IUBMB Life*, **61**, 91–98, 2009.
[15] Freeman, B.A., Baker, P.R., Schopfer, F.J., Woodcock, S.R., Napolitano, A., and d'Ischia, M.: Nitro-fatty acid formation and signaling. *J. Biol. Chem.*, **283**, 15515–15519, 2008.
[16] Stamler, J.S., Lamas, S., and Fang, F.C.: Nitrosylation. the prototypic redox-based signaling mechanism. *Cell*, **106**, 675–683, 2001.
[17] Eiserich, J.P., Hristova, M., Cross, C.E., Jones, A.D., Freeman, B.A., Halliwell, B., and van der Vliet, A.: Formation of nitric oxide-derived inflammatory oxidants by myeloperoxidase in neutrophils. *Nature*, **391**, 393–397, 1998.
[18] Schopfer, F.J., Baker, P.R., and Freeman, B.A.: NO-dependent protein nitration: a cell signaling event or an oxidative inflammatory response? *Trends Biochem. Sci.*, **28**, 646–654, 2003.
[19] Radi, R.: Nitric oxide, oxidants, and protein tyrosine nitration. *Proc. Natl. Acad. Sci. U.S.A.*, **101**, 4003–4008, 2004.
[20] Terasaki, Y., Akuta, T., Terasaki, M., Sawa, T., Mori, T., Okamoto, T., Ozaki, M., Takeya, M., and Akaike, T.: Guanine nitration in idiopathic pulmonary fibrosis and its implication for carcinogenesis. *Am. J. Respir. Crit. Care Med.*, **174**, 665–673, 2006.
[21] Yoshitake, J., Akaike, T., Akuta, T., Tamura, F., Ogura, T., Esumi, H., and Maeda, H.: Nitric oxide as an endogenous mutagen for Sendai virus without antiviral activity. *J. Virol.*, **78**, 8709–8719, 2004.
[22] Sawa, T., Zaki, M.H., Okamoto, T., Akuta, T., Tokutomi, Y., Kim-Mitsuyama, S., Ihara, H., Kobayashi, A., Yamamoto, M., Fujii, S., Arimoto, H., and Akaike, T.: Protein *S*-guanylation by the biological signal 8-nitroguanosine 3',5'-cyclic monophosphate. *Nat. Chem. Biol.*, **3**, 727–735, 2007.
[23] Zaki, M.H., Fujii, S., Okamoto, T., Islam, S., Khan, S., Ahmed, K.A., Sawa, T., and Akaike, T.: Cytoprotective function of heme oxygenase 1 induced by a nitrated cyclic nucleotide formed during murine salmonellosis. *J. Immunol.*, **182**, 3746–3756, 2009.
[24] D'Autreaux, B. and Toledano, M.B.: ROS as signalling molecules: mechanisms that generate specificity in ROS homeostasis. *Nat. Rev. Mol. Cell Biol.*, **8**, 813–824, 2007.
[25] Bove, P.F. and van der Vliet, A.: Nitric oxide and reactive nitrogen species in airway epithelial signaling and inflammation. *Free Radic. Biol. Med.*, **41**, 515–527, 2006.
[26] Ricciardolo, F.L., Di Stefano, A., Sabatini, F., and Folkerts, G.: Reactive nitrogen species in the respiratory tract. *Eur. J. Pharmacol.*, **533**, 240–252, 2006.
[27] Alam, J. and Cook, J.L.: How many transcription factors does it take to turn on the heme oxygenase-1 gene? *Am. J. Respir. Cell Mol. Biol.*, **36**, 166–174, 2007.
[28] Balla, G., Jacob, H.S., Balla, J., Rosenberg, M., Nath, K., Apple, F., Eaton, J.W., and Vercellotti, G.M.: Ferritin: a cytoprotective antioxidant strategem of endothelium. *J. Biol. Chem.*, **267**, 18148–18153, 1992.
[29] Stocker, R., Yamamoto, Y., McDonagh, A.F., Glazer, A.N., and Ames, B.N.: Bilirubin is an antioxidant of possible physiological importance. *Science*, **235**, 1043–1046, 1987.
[30] Ryter, S.W., Alam, J., and Choi, A.M.: Heme oxygenase-1/carbon monoxide: from basic science to therapeutic applications. *Physiol. Rev.*, **86**, 583–650, 2006.
[31] Srisook, K., Kim, C., and Cha, Y.N.: Role of NO in enhancing the expression of HO-1 in LPS-stimulated macrophages. *Methods Enzymol.*, **396**, 368–377, 2005.
[32] Motohashi, H. and Yamamoto, M.: Nrf2-Keap1 defines a physiologically important stress response mechanism. *Trends Mol. Med.*, **10**, 549–557, 2004.
[33] Dinkova-Kostova, A.T., Holtzclaw, W.D., and Kensler, T.W.: The role of Keap1 in cellular protective responses. *Chem. Res. Toxicol.*, **18**, 1779–1791, 2005.
[34] Dinkova-Kostova, A.T., Holtzclaw, W.D., Cole, R.N., Itoh, K., Wakabayashi, N., Katoh, Y., Yamamoto, M., and Talalay, P.: Direct evidence that sulfhydryl groups of Keap1 are the sensors regulating induction of phase 2 enzymes that protect against carcinogens and oxidants. *Proc. Natl. Acad. Sci. U.S.A.*, **99**, 11908–11913, 2002.
[35] Wakabayashi, N., Dinkova-Kostova, A.T., Holtzclaw, W.D., Kang, M.I., Kobayashi, A., Yamamoto, M., Kensler, T.W., and Talalay, P.: Protection against electrophile and oxidant stress by induction of the phase 2 response: fate of cysteines of the Keap1 sensor modified by inducers. *Proc. Natl. Acad. Sci. U.S.A.*, **101**, 2040–2045, 2004.
[36] Itoh, K., Tong, K.I., and Yamamoto, M.: Molecular mechanism activating Nrf2-Keap1 pathway in regulation of adaptive response to electrophiles. *Free Radic. Biol. Med.*, **36**, 1208–1213, 2004.
[37] Takaya, A., Suzuki, A., Kikuchi, Y., Eguchi, M., Isogai, E., Tomoyasu, T., and Yamamoto, T.: Derepression of *Salmonella* pathogenicity island 1 genes within macrophages leads to rapid apoptosis via caspase-1- and caspase-3-dependent pathways. *Cell. Microbiol.*, **7**, 79–90, 2005.
[38] Wiesel, P., Patel, A.P., DiFonzo, N., Marria, P.B., Sim, C.U., Pellacani, A., Maemura, K., LeBlanc, B.W., Marino, K., Doerschuk, C.M., Yet, S.F., Lee, M.E., and Perrella, M.A.: Endotoxin-induced mortality is related to increased oxidative stress and end-organ dysfunction, not refractory hypotension, in heme oxygenase-1-deficient mice. *Circulation*, **102**, 3015–3022, 2000.
[39] Poss, K.D. and Tonegawa, S.: Reduced stress defense in heme oxygenase 1-deficient cells. *Proc. Natl. Acad. Sci. U.S.A.*, **94**, 10925–10930, 1997.

Am J Physiol Renal Physiol 298: F133–F141, 2010.
First published November 11, 2009; doi:10.1152/ajprenal.00400.2009.

Histone deacetylase modulates the proinflammatory and -fibrotic changes in tubulointerstitial injury

Takeshi Marumo,[1,2] Keiichi Hishikawa,[1,2] Masahiro Yoshikawa,[1,2] Junichi Hirahashi,[2] Shoji Kawachi,[3] and Toshiro Fujita[1,2]

[1]*Department of Clinical Renal Regeneration,* [2]*Division of Nephrology and Endocrinology, Department of Internal Medicine, University of Tokyo, and* [3]*Surgical Operation Department, International Medical Center of Japan, Tokyo, Japan*

Submitted 15 July 2009; accepted in final form 4 November 2009

Marumo T, Hishikawa K, Yoshikawa M, Hirahashi J, Kawachi S, Fujita T. Histone deacetylase modulates the proinflammatory and -fibrotic changes in tubulointerstitial injury. *Am J Physiol Renal Physiol* 298: F133–F141, 2010. First published November 11, 2009; doi:10.1152/ajprenal.00400.2009.—Histone deacetylase (HDAC) regulates gene expression by modifying chromatin structure. Although changes in the expression and activities of HDAC may affect the course of kidney disease, the role of HDAC in tubulointerstitial injury has not been explored. We therefore investigated the alterations in HDAC expression and determined the effects of HDAC inhibition on the tubulointerstitial injury induced by unilateral ureteral obstruction. The induction of HDAC1 and HDAC2, accompanied by a decrease in histone acetylation was observed in kidneys injured by ureteral obstruction. Immunohistochemical analysis revealed that HDAC1 and HDAC2 were induced in renal tubular cells. Treatment with an HDAC inhibitor, trichostatin A (TSA), attenuated macrophage infiltration and fibrotic changes in tubulointerstitial injury induced by ureteral obstruction. The induction of colony-stimulating factor-1 (CSF-1), a chemokine known to be involved in macrophage infiltration in tubulointerstitial injury, was reduced in injured kidneys from mice treated with TSA. TSA, valproate, and the knockdown of HDAC1 or HDAC2 significantly reduced CSF-1 induced by TNF-α in renal tubular cells. These results suggest that tubular HDAC1 and HDAC2, induced in response to injury, may contribute to the induction of CSF-1 and the initiation of macrophage infiltration and profibrotic responses. These findings suggest a potential of HDAC inhibition therapy aimed at reducing inflammation and fibrosis in tubulointerstitial injury.

epigenetic; chemokine; ureteral obstruction

EPIGENETIC MECHANISMS INCLUDING changes in histone acetylation have recently been suggested to be involved in altered gene expression in various pathological conditions, including cancer (33), cardiac hypertrophy (4), chronic obstructory pulmonary disease (14), denervation (24), and recovery of learning and memory after neuronal loss (10). Changes in histone acetylation, which are controlled by histone deacetylase (HDAC) and histone acetyltransferase, regulate gene transcription by altering chromatin structure. The distinct roles of each HDAC isozyme in such pathological conditions have recently begun to be revealed (11, 12, 28, 29, 36). Despite the potential role of HDAC in molecular responses to kidney injury, changes in the expression of HDAC and histone acetylation in the kidney have not been characterized. In this regard, we recently reported that HDAC5 downregulation, which leads to histone acetylation in renal tubular cells, contributes to the regenerative response to ischemia (21).

The importance of changes in HDAC activity and histone acetylation in kidney disease has also been indicated by the observations by us and others that the HDAC inhibitor reduced glomerular lesions and proteinuria in models of lupus nephritis (26) and anti-glomerular basement membrane glomerulonephritis (13). In addition to glomerulonephritis, our previous in vitro observation suggested that tubulointerstitial injury can also be a direct target of HDAC inhibitors independently of glomerular lesions, since an HDAC inhibitor, trichostatin A (TSA), attenuates the epithelial-to-mesenchymal transition induced by transforming growth factor (TGF)-β in cultured renal tubular cells (42).

The infiltration of inflammatory cells into the interstitial space in the kidney is one of the earliest events in tubulointerstitial injury and regulates fibrosis and tubular atrophy (1, 8). In response to injury, renal tubular cells express several chemokines that induce the migration of inflammatory cells into the interstitium. Although the contribution of a subset of macrophages in the resolution of renal injury needs to be clarified in each pathological condition (31), the inhibition of initial macrophage influx by the blockade of some of the intrarenal chemokines, such as monocyte chemoattractant protein (MCP)-1 (2, 19) and colony-stimulating factor (CSF)-1 (16, 20), has been shown to attenuate tubulointerstitial injury induced by ureteral obstruction.

In the present study, we investigated the changes in HDAC expression and histone acetylation in kidney injured by unilateral ureteral obstruction (UUO), a model of tubulointerstitial injury characterized by inflammation and fibrosis that is independent of glomerular lesions. We further determined the effects of HDAC inhibition on the early stages of inflammatory and fibrotic changes induced by UUO.

MATERIALS AND METHODS

UUO injury. Seven- to eight-week-old male C57BL/6J mice (Tokyo Laboratory Animal Center, Tokyo, Japan) were fed a standard laboratory diet (MF; Oriental Yeast, Tokyo, Japan) and water ad libitum. The left ureter was exposed through the flank and completely ligated with 4.0 silk under anesthesia with pentobarbital sodium (50 mg/kg ip). Mice were randomly assigned to two groups and were treated as follows. The TSA-treated group was composed of animals treated with 10 mg/kg of TSA, which was administered by intraperitoneal injection daily for 2 or 5 days. The vehicle-treated group was composed of animals treated with dimethylsulfoxide instead of TSA. Two or five days after UUO, the kidneys were perfused with saline and removed from animals under anesthesia with pentobarbital sodium. For the morphological analysis and immunohistochemical analysis of α-smooth muscle actin (SMA), a marker of myofibroblasts,

Address for reprint requests and other correspondence: T. Marumo, Dept. of Clinical Renal Regeneration, and Div. of Nephrology and Endocrinology, Dept. of Internal Medicine, Univ. of Tokyo, 7-3-1 Hongo, Bunkyo-ku, 113-8655 Tokyo, Japan (e-mail: tmarumo-npr@umin.ac.jp).

Table 1. *Primer sequences for RT-PCR*

Primer	Sequence of PCR Primers	GenBank Accession No.
Mouse HDAC1		NM_008228
Forward	5′-CTCAGGGCACCAAGAGGAAAG-3′	
Reverse	5′-TTGAGCAGCAAATTGTGAGTCA-3′	
Mouse HDAC2		NM_008229
Forward	5′-TGCTTGCCATCCTCGAATTACT-3′	
Reverse	5′-GTCATCACGCGATCTGTTGTATAAA-3′	
Mouse HDAC3		NM_010411
Forward	5′-GCCTTCAACGTGGGTGATG-3′	
Reverse	5′-CCTGTGTAACGGGAGCAGAAC-3′	
Mouse HDAC4		NM_207225
Forward	5′-GATCCTCATTGTAGACTGGGATGTAC-3′	
Reverse	5′-ATAGCGGTGCAGGGACATGTA-3′	
Mouse HDAC6		NM_010413
Forward	5′-AAAAGAAGCACCGCATTCAGA-3′	
Reverse	5′-GTTCATATCGGTGGATGGAGAAA-3′	
Mouse HDAC7		NM_019572
Forward	5′-GACCCCAGTGTGCTCTACATTTC-3′	
Reverse	5′-TGCCAGTTCCCACCTCATC-3′	
Mouse collagen Ia		NM_007742
Forward	5′-GCCTTGGAGGAAACTTTGCTT-3′	
Reverse	5′-GCACGGAAACTCCAGCTGAT-3′	
Mouse α-SMA		NM_007392
Forward	5′-CACGGCATCATCACCAACTG-3′	
Reverse	5′-GGCCACACGAAGCTCGTTAT-3′	
Mouse CSF-1		NM_007778
Forward	5′-GGGGTGGAAGACATTCTTGA-3′	
Reverse	5′-TGTCAGTCTCTGCCTGGATG-3′	
Mouse EMR-1		NM_010130
Forward	5′-TGGCTGCCTCCCTGACTTT-3′	
Reverse	5′-ATTGCTGTATCTGCTCACTTTGGA-3′	
Mouse MCP-1		NM_011333
Forward	5′-GCAGTTAACGCCCCACTCA-3′	
Reverse	5′-CCTACTCATTGGGATCATCTTGCT-3′	
Rat CSF-1		NM_023981
Forward	5′-CATCCAGGCAGAGACTGACA-3′	
Reverse	5′-TGTCAACGGGGTGTCTGTTA-3′	
Rat HDAC1		XM_576595
Forward	5′-AATTTGCTGCTCAACTATGGTCTCT-3′	
Reverse	5′-TGATGTAGTCGTCGCTGTGGTACT-3′	
Rat HDAC2		XM_342149
Forward	5′-CCATGGCGTACAGTCAAGGA-3′	
Reverse	5′-AATAATTCCCGATATCACCGTCATA-3′	

HDAC, histone deacetylase; SMA, smooth muscle actin; CSF-1, colony-stimulating factor 1; EMR-1, epidermal growth factor-like molecule containing mucin-like hormone receptor 1; MCP-1, monocyte chemoattractant protein 1.

coronal sections of renal tissue were immersion-fixed in 10% neutral-buffered formalin and embedded in paraffin. The right kidneys from the same mice were examined as samples of kidneys not subjected to injury. Animal care and treatment complied with the standards described in the Guidelines for the Care and Use of Laboratory Animals of the University of Tokyo.

Renal morphology. To investigate morphological changes, 4-μm paraffin sections were stained by the Masson's trichrome method and examined by light microscopy. Images were obtained with a digital camera (DXM 1200C, Nikon, Tokyo, Japan). Interstitial fibrosis was scored semiquantitatively as previously reported (9) and graded as follows: 0, no staining; 1+, mild staining; 2+, moderate staining; 3+, marked staining; and 4+, severe staining. At least 10 different cortical fields (×200) were randomly selected from each specimen by one of the authors, who was unaware of the origin of the slides.

Immunohistochemistry. For the immunohistochemical staining of HDAC1, HDAC2, acetylated histone H3, and F4/80, a marker of macrophages which is also designated epidermal growth factor-like molecule containing mucin-like hormone receptor 1 (EMR-1), in the renal tissue, coronal sections of the renal tissue were immersion-fixed in 4% buffered-paraformaldehyde for 12 h, washed with 10, 15, and 20% sucrose in PBS for 4 h each time, embedded in Optimal Cutting Temperature compound, and snap-frozen in liquid nitrogen. Frozen sections, 6 μm in thickness, were stained with rabbit anti-HDAC1 polyclonal antibody (dilution 1:100, Lab Vision Products, Thermo Fisher Scientific, Fremont, CA), rabbit anti-HDAC2 polyclonal antibody (dilution 1:50, Santa Cruz Biotechnology, Santa Cruz, CA), rabbit anti-acetylated histone H3 (Lys9) polyclonal antibody (dilution 1:300, Upstate Biotechnology), and rat anti-F4/80 monoclonal antibody (dilution 1:100, Serotec, Oxford, UK), as the respective primary antibodies. For HDAC1, HDAC2, and acetylated histone H3, Alexa Fluor 488 goat anti-rabbit IgG (Molecular Probes, Eugene, OR) was used as the secondary antibody at a dilution of 1:200. Slides were mounted with Vectashield antifade mounting medium with DAPI

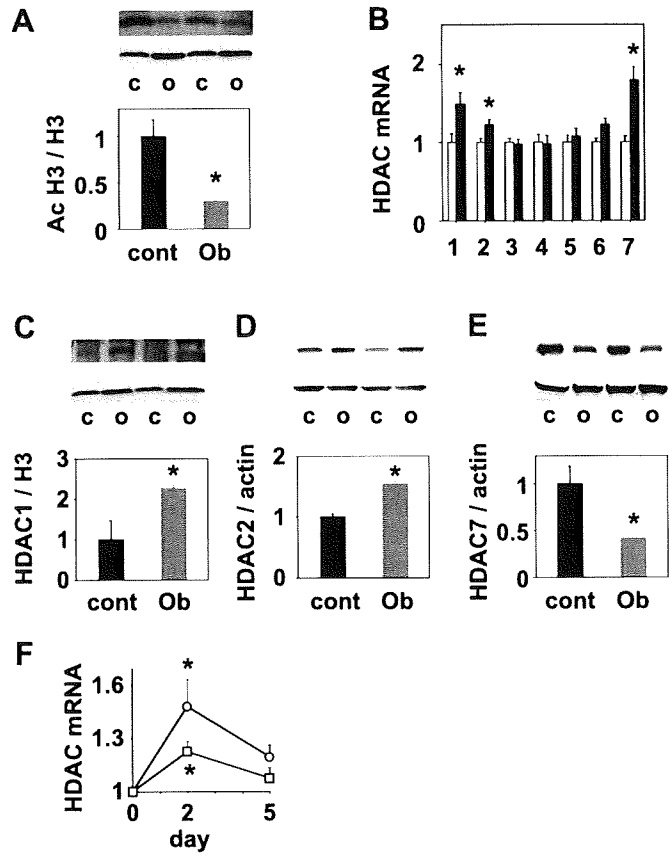

Fig. 1. Decrease in histone acetylation and induction of histone deacetylase (HDAC) 1 and HDAC2 by unilateral ureteral obstruction (UUO) for 2 days. *A*: representative films of Western blot analysis for acetylated histone and actin obtained from contralateral (c or cont) and obstructed (o or Ob) kidneys (*top* and *middle*, respectively). The results of densitometric analysis are shown at the *bottom*. Values are means ± SE (n = 5). *P < 0.05 vs. values of contralateral kidneys. *B*: changes in the mRNA levels of HDAC isozymes determined by RT-PCR are shown. Values of contralateral (open bars) and obstructed (filled bars) kidneys were normalized to those for 18S and expressed as relative values of contralateral kidneys. Values are means ± SE (n = 4–8). *P < 0.05 vs. values of contralateral kidneys. *C–E*: representative films of Western blot analysis for HDAC1 (*C*), HDAC2 (*D*), and HDAC7 (*E*) obtained from contralateral (c or cont) and obstructed (o or Ob) kidneys are shown (*top*). Blots for histone H3 (*C*) and actin (*D* and *E*) are also shown (*middle*). The results of densitometric analysis are shown at the *bottom*. Values are means ± SE (n = 4–5). *P < 0.05 vs. values of contralateral kidneys. *F*: time course of increase in HDAC. HDAC1 (○) and HDAC2 (□) mRNA levels of obstructed kidneys were normalized to values for 18S and expressed as relative values of contralateral kidneys. Values are means ± SE (n = 4–8). *P < 0.05 vs. values of contralateral kidneys.

(Vector Laboratories, Burlingame, CA). Images were obtained with a digital camera (DXM 1200C, Nikon) attached to an Eclipse E600 epifluorescence microscope (Nikon). For determination of the percentage of cells positive for acetylated histone, HDAC1, and HDAC2, at least eight different fields in the cortex of each kidney, each containing at least 50 proximal tubular cells, were analyzed. For the detection of F4/80, immobilized antibody was detected using the biotin-avidin-immunoperoxidase technique with a Vectastain ELIT ABC kit (Vector Laboratories) and 3–3′-diaminobenzidine as the chromogen. Sections were then counterstained with Mayer's hematoxylin and examined by light microscopy. The number of F4/80-positive cells in the cortical area was counted in a blinded fashion in at least 10 different cortical fields (×200) for each section, and the mean values per section were calculated. For the detection of α-SMA, deparaffinized sections, 4 μm thick, were stained with mouse anti-α-SMA monoclonal antibody (1:50 dilution, 1A4, Dako), according to a method previously described (37). Immobilized antibody was detected using the biotin-avidin-immunoperoxidase technique with a Vectastain ELIT ABC kit (Vector Laboratories) and 3–3′-diaminobenzidine as the chromogen. Sections were then counterstained with Mayer's hematoxylin and examined by light microscopy. The ratio of the interstitial α-SMA-positive area to the cortical area was calculated by image analysis using a Nikon ACT-1C, Adobe Photoshop 7.0, and Scion Image. The mean value of the α-SMA-positive area was obtained by evaluating at least 10 different cortical fields (×200) from each kidney in a blinded manner. Negative controls for all the immuno-

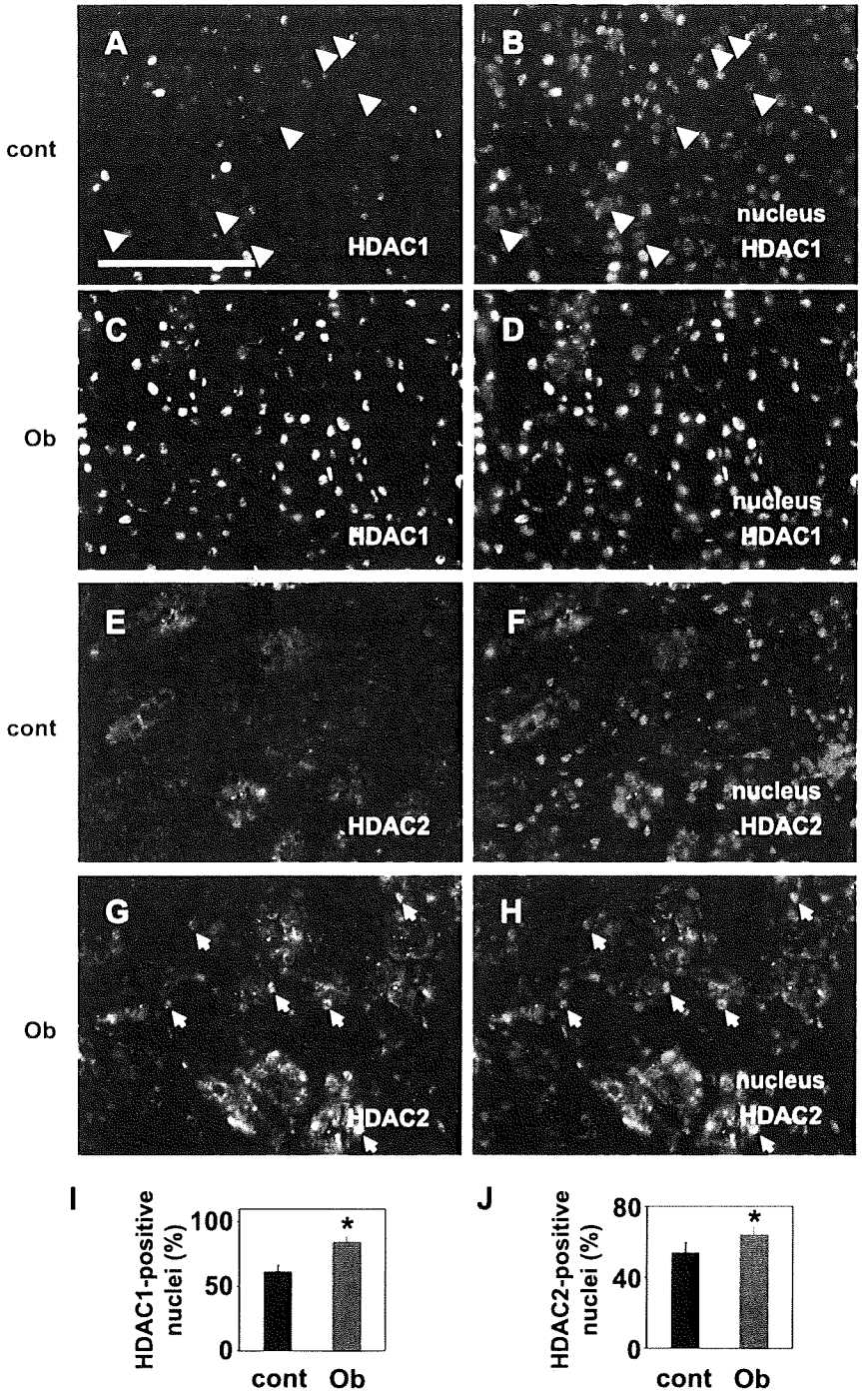

Fig. 2. Increase in tubular expression of HDAC1 and HDAC2 by UUO. Immunohistochemical staining of the renal cortex from contralateral (*A*, *B*, *E*, and *F*) and obstructed (*C*, *D*, *G*, and *H*) kidneys with HDAC1 (*A–D*) and HDAC2 (*E–H*) at 2 days after obstruction is shown in green. Localization of nuclei in the same sections (*A*, *C*, *E*, and *G*) is shown by costaining with DAPI (red) in panels *B*, *D*, *F*, and *H*, respectively. Bar = 100 μm. Nuclei stained negative for HDAC1 are shown by arrowheads in *A* and *B*. Nuclei stained positive for HDAC2 are shown by arrows in *G* and *H*. Quantitative analysis of nuclei positive for HDAC1 (*I*) and HDAC2 (*J*) in the cortex of contralateral and obstructed kidneys is shown. Values are means ± SE expressed as a percentage of total nuclei (n = 4–5). *$P < 0.05$ vs. values of contralateral kidneys.

histochemical stainings were obtained by substitution of the primary antibody with PBS or normal IgG.

Western blotting. Renal tissue was immediately snap-frozen in liquid nitrogen and stored at −70°C and further processed according to a previously described method (6, 13). After determination of the protein concentrations of the lysates with a protein assay kit (Bio-Rad, Richmond, CA), equal amounts of protein (100 μg) were immunoblotted with rabbit anti-acetyl histone H3 (Lys9) polyclonal antibody (Upstate Biotechnology), HDAC1 (Sigma), HDAC2 (Santa Cruz Biotechnology), HDAC7 (Sigma), or α-SMA (Dako) and analyzed using standard SDS-PAGE and Western blotting (22). For the detection of HDAC1, the nuclear protein was used to reduce nonspecific bands observed in blots using the whole tissue extract. The nuclear protein was extracted using a Nuclear/Cytosol Fraction Kit (BioVision Research Products, Mountain View, CA) in accordance with the manufacturer's instructions. β-Actin (41) and H3 (23, 27) were used as the loading controls for whole cell lysate and nuclear protein, respectively. The values obtained by densitometric analysis of Western blots were normalized to those for actin or histone H3 and expressed as relative values to those of control.

Analysis of mRNA levels. Total RNA was extracted from renal tissue or NRK 52E with an RNA extraction kit, RNeasy Mini (Qiagen, Tokyo, Japan). The cDNA product was generated using a high-capacity cDNA archive kit (Applied Biosystems, Foster City, CA). The expression levels of HDAC isozymes, collagen 1a, α-SMA, EMR-1, MCP-1, and CSF-1 were analyzed with the ABI 7500 sequence detection system using SYBR Green PCR Master Mix (Applied Biosystems). Primer sequences are shown in Table 1. For detection of mouse HDAC5 and 18S ribosomal RNA, primers and probes were obtained from Applied Biosystems, and Taqman Universal PCR Master Mix was used. The thermal cycling parameters were 95°C for 10 min for AmpliTaq Gold activation, followed by 40 cycles of 15 s at 95°C for denaturation, and 1 min at 60°C for annealing/extension. Values were normalized to the

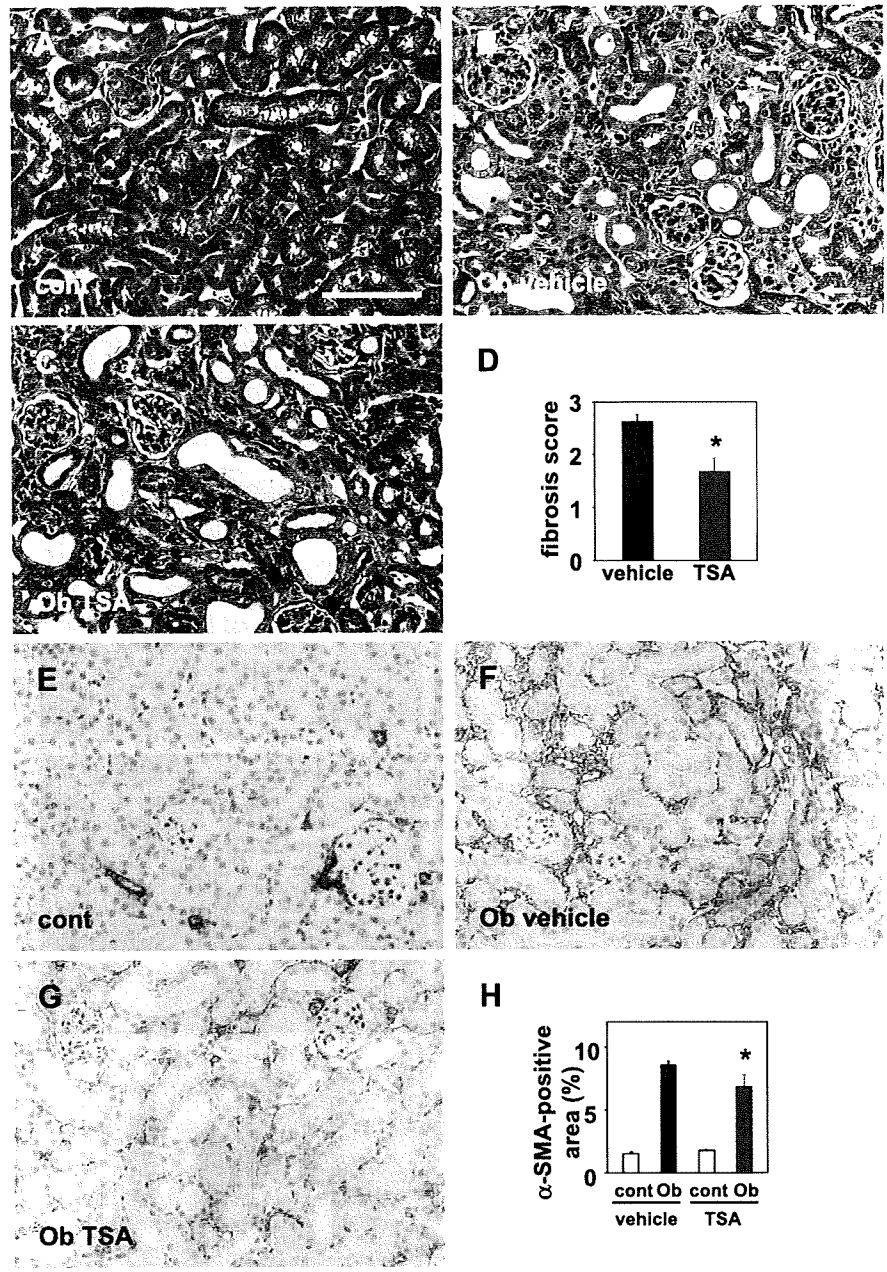

Fig. 3. Attenuation of tubulointerstitial fibrosis in UUO mice by HDAC inhibition. Representative photomicrographs of Masson's trichrome staining (*A–C*) and α-smooth muscle action (SMA) staining (*E–G*) of the contralateral (*A* and *E*) and injured (*B*, *C*, *F*, and *G*) kidneys. The UUO mice received intraperitoneal injections of vehicle (*A*, *B*, *E*, and *F*) or trichostatin A (TSA; *C* and *G*). Kidney sections were obtained 5 days after ureteral obstruction. Expansion of interstitial space by extracellular matrix and inflammatory cells observed in *B* (arrows) was reduced (*C*). Values are means ± SE of the average interstitial fibrosis score and α-SMA-positive area, respectively, from 5 mice that had received the intraperitoneal injections of vehicle or TSA. Bar = 100 μm. *$P < 0.05$ vs. values of obstructed kidneys obtained from mice treated with vehicle.

levels of 18S rRNA and expressed as relative values to those obtained with control.

Renal tubular cell culture and RNA interference for knockdown of HDAC1 and HDAC2. The normal rat kidney epithelium-derived cell line NRK 52E was obtained from the American Type Culture Collection and grown in DMEM with 5% FBS in a humidified 5% CO_2-95% air environment at 37°C. Subconfluent NRK 52E cells were transfected with 33 nM HDAC1 or HDAC2 Stealth RNAi (RNA interference; Invitrogen Japan, Tokyo, Japan), or Stealth RNAi Negative Control Duplex (Lo GC Duplex, Invitorgen) using Lipofectamine RNAiMAX (Invitrogen) in accordance with the manufacturer's instructions. The sequences employed were as follows: HDAC1 sense, 5′-CGGCAUUGAUGAUGAGUCCUAUGAA-3′, antisense, 5′-UUCAUAGGACUCAUCAUCAAUGCCG-3′; and HDAC2 sense, 5′-CCUAACUGUCAAAGGUCACGCUAAA-3′, antisense, 5′-UUUAGCGUGACCUUUGACAGUUAGG-3′. After 24 h of incubation with the RNAi, cells were then treated with or without TNF-α for 24 h.

Statistics. All data are expressed as means ± SE. Multiple parametric comparisons were performed by analysis of variance, followed by Fisher's protected least significant difference test. Comparisons between two groups were performed by Student's *t*-test. Values of $P < 0.05$ were considered statistically significant.

RESULTS

Decrease in histone acetylation accompanied by an increase in HDAC1 and HDAC2 in injured kidneys. UUO-induced kidney injury produced a marked decrease in the level of histone acetylation compared with that in the contralateral kidneys (Fig. 1*A*). Since HDACs are major determinants of histone acetylation levels, we analyzed the changes in the mRNA levels of HDACs in the injured kidneys. The mRNA levels of HDAC1, HDAC2, and HDAC7 were increased in the injured kidneys, whereas those of HDAC3, HDAC4, HDAC5, and HDAC6 remained unchanged compared with those in the contralateral kidneys (Fig. 1*B*). In parallel with the changes in the mRNA levels, the protein levels of HDAC1 and HDAC2 increased in the obstructed kidneys (Fig. 1, *C* and *D*). These observations suggest that the upregulation of HDAC1 and HDAC2 may, at least in part, be involved in a decrease in histone acetylation level in the injured kidneys. In contrast to HDAC1 and HDAC2, however, the HDAC7 protein level was paradoxically decreased in the injured kidneys (Fig. 1*E*). The cause of this discrepancy between the HDAC7 mRNA and protein levels is unknown, but we suspect the possible degradation of HDAC7 protein and the subsequent upregulation of mRNA through a feedback mechanism in the injured kidneys. While further investigation of these changes in HDAC7 is of interest, we rather decided to concentrate on the upregulation of HDAC1 and HDAC2 in the present report, as these changes may contribute to histone deacetylation in the injured kidneys. Induction of HDAC1 and HDAC2 mRNA was estimated to occur in the early stage of injury since the mRNA levels reached the peak at 2 days after UUO treatment (Fig. 1*F*).

To determine the intrarenal changes in HDAC1 and HDAC2, we next performed immunohistochemical analysis. The expression of HDAC1 was observed in the nuclei of tubular and glomerular cells in uninjured kidneys, but some tubular cells did not stain positive for HDAC1 (Fig. 2, *A* and *B*, arrowheads). In contrast, strong staining for HDAC1 was observed in the tubular cells of the injured kidneys (Fig. 2, *C* and *D*). HDAC1 negative cells were rarely observed in the tubular cells of the injured kidneys. HDAC2 staining was less pronounced than HDAC1 staining, but significant HDAC2 staining was observed in the nuclei of tubular and glomerular cells in the contralateral kidneys (Fig. 2, *E* and *F*). In the injured kidneys, strong HDAC2 staining was observed in some tubular cells (Fig. 2, *G* and *H*, arrows). Cell counting analysis revealed that the percentage of tubular cells positive for HDAC1 and HDAC2 was significantly increased in the injured kidneys compared with that in the contralateral kidneys (Fig. 2, *I* and *J*). These observations indicate that HDAC1 and HDAC2 are induced in tubular cells in response to UUO.

Histone deacetylase inhibitor ameliorates fibrotic changes. Based on the results that histone deacetylation and the upregulation of HDAC1 and HDAC2 are induced in the early stage of UUO, we next determined the effects of an HDAC inhibitor, TSA, on the early fibrotic changes observed in the injured kidneys. TSA markedly decreased the interstitial fibrosis induced by UUO (Fig. 3, *A–C*). The fibrosis score was significantly reduced in the obstructed kidneys of the mice treated with TSA compared with the samples obtained from animals treated with vehicle (Fig. 3*D*). In accordance with the results obtained using Masson's trichrome staining, the area positive for α-SMA was significantly reduced by TSA treatment (Fig. 3, *E–H*). Western blot analysis revealed that the protein levels of α-SMA in obstructed kidneys were attenuated by ~15% in TSA-treated mice (Fig. 4*A*). In addition, an increase in the mRNA level of collagen 1a and α-SMA induced by UUO was significantly attenuated by TSA (Fig. 4, *B* and *C*). TSA treat-

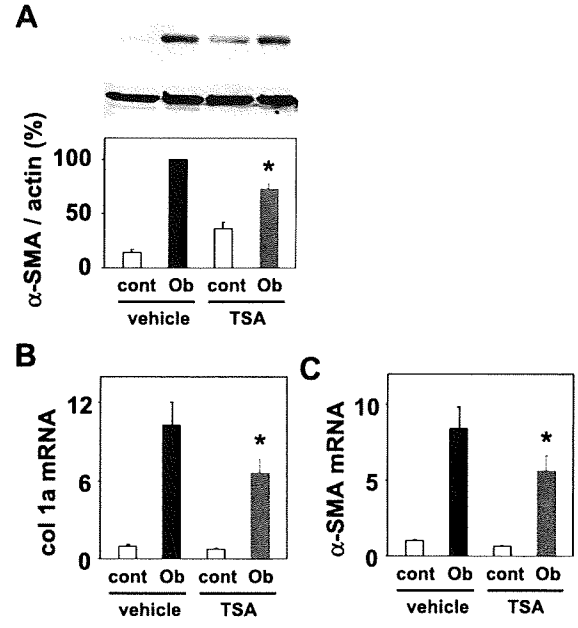

Fig. 4. Reduction in fibrotic markers in UUO mice by HDAC inhibition. The protein levels of α-SMA (*A*) in kidneys obtained 2 days after ureteral obstruction from mice treated with vehicle or TSA were determined by Western blot analysis. Representative films of Western blot analysis for α-SMA are shown at the *top*. Blots for β-actin are shown in the *middle*. The results of densitometric analysis are shown at the *bottom*. Values are means ± SE ($n = 4$). The mRNA levels of collagen 1a (*B*) and α-SMA (*C*) in kidneys obtained 2 days after ureteral obstruction from mice treated with vehicle or TSA were determined by RT-PCR. Values were normalized to those for 18S and expressed as relative values of contralateral kidneys obtained from mice treated with vehicle. Values are means ± SE ($n = 7–8$). *$P < 0.05$ vs. values of obstructed kidneys obtained from mice treated with vehicle.

ment indeed increased the level of histone acetylation of renal tubular cells, as judged from the observation that while there were some tubular cells negative for histone acetylation staining in obstructed kidneys obtained from mice treated with vehicle (Fig. 5, *A* and *B*, arrowheads), most of the tubular cells in the obstructed kidneys obtained from mice treated with TSA were positive for acetylated histone (Fig. 5, *C* and *D*). Tubular cells positive for nuclear staining with acetylated histone was significantly increased in TSA-treated animals (Fig. 5*E*).

HDAC inhibitor attenuates inflammation. We next examined the effects of HDAC inhibition on the macrophage infiltration and chemokine expression induced by UUO. Macrophage infiltration and the increase in mRNA levels of EMR-1 (F4/80), a marker of macrophages, were significantly reduced in the obstructed kidneys obtained from mice treated with TSA compared with those in kidneys obtained from mice treated with vehicle (Fig. 6, *A* and *B*). Since MCP-1 and CSF-1 have been shown to mediate macrophage infiltration in the early phase of UUO (2, 16, 19, 20), we determined the effects of HDAC inhibitor on the mRNA levels of these chemokines. While the induction of MCP-1 mRNA was not altered, the increase in the level of CSF-1 mRNA was significantly lower in the obstructed kidneys of TSA-treated mice than in those of mice treated with vehicle (Fig. 6, *C* and *D*). These results suggest that TSA may attenuate inflammation, at least in part, by inhibiting induction of CSF-1 but not MCP-1.

Involvement of HDAC1 and HDAC2 in CSF-1 expression in tubular cells. To gain further insight into the role of HDAC in CSF-1 induction, we next used rat tubular epithelial cells (NRK 52E). Stimulation of the tubular cells with TNF-α, a cytokine involved in renal injury induced by UUO (5), significantly induced CSF-1 mRNA (Fig. 7*A*). In accordance with the results obtained in UUO, TSA attenuated the induction of CSF-1 (Fig. 7*A*), while it had no effects on MCP-1 induction (Fig. 7*B*). Valproate, another HDAC inhibitor, also reduced CSF-1 induction by TNF-α (Fig. 7*C*). These results indicate that HDAC indeed plays a critical role in CSF-1 induction in renal tubular cells. To delineate the possible roles of HDAC1 and HDAC2 on CSF-1 induction, we knocked down the expression of HDACs using RNA interference (RNAi). The HDAC1 mRNA level was markedly reduced following the transfection of HDAC1 Stealth RNAi, compared with that of cells transfected with control Stealth RNAi [HDAC1 Stealth RNAi (0.16 ± 0.01 arbitrary units) vs. control Stealth RNAi (1.00 ± 0.20 arbitrary units; $P < 0.05$; $n = 8$)]. The induction of CSF-1 by TNF-α was prevented by the downregulation of HDAC1 (Fig. 7*D*). The knockdown of HDAC2 by HDAC2 Stealth RNAi [HDAC2 Stealth RNAi (0.10 ± 0.01 arbitrary units) vs. control Stealth RNAi (1.00 ± 0.17 arbitrary units, $P < 0.05$, $n = 8$)] also reduced CSF-1 induction by TNF-α, although the reduction in CSF-1 mRNA was less pronounced than that achieved by HDAC1 knockdown (Fig. 7*E*). These results indicate the important roles of HDAC1 and HDAC2 in the expression of CSF-1 in tubular cells stimulated with TNF-α.

DISCUSSION

Accumulating evidence indicates that the changes in HDAC expression and histone acetylation are involved in transmission

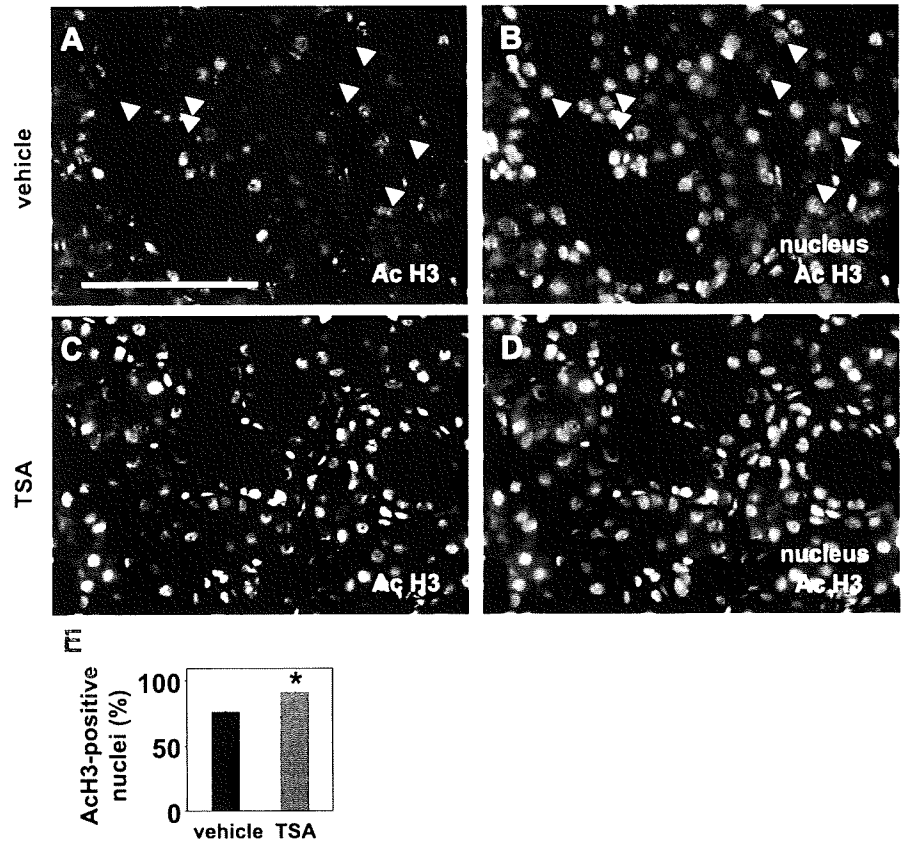

Fig. 5. Representative photomicrographs of staining with acetylated histone of the injured kidneys obtained from mice treated with vehicle (*A* and *B*) or TSA (*C* and *D*). Samples were obtained on *day 2*. Localization of nuclei in the same sections (*A* and *C*) is shown by costaining with DAPI (red) in *B* and *D*, respectively. Nuclei stained negative for acetylated histone are shown by arrowheads in *A* and *B*. *E*: quantitative analysis of tubular cells positive for acetylated histone in the injured kidneys obtained from mice treated with vehicle or TSA. Values are means ± SE expressed as a percentage of total nuclei ($n = 5$). Bar = 100 μm.*$P < 0.05$ vs. values of obstructed kidneys obtained from mice treated with vehicle.

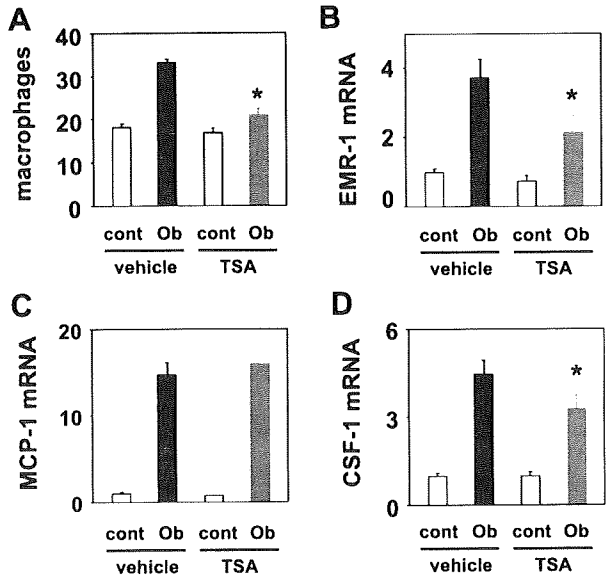

Fig. 6. Reduction in infiltration of macrophages and colony-stimulating factor (CSF)-1 mRNA levels in UUO mice by HDAC inhibition. *A*: mean number of F4/80-positive cells in the interstitium of the kidneys obtained 2 days after ureteral obstruction is indicated as means ± SE (n = 5). *P < 0.05 vs. values of obstructed kidneys obtained from mice treated with vehicle. The mRNA levels of epidermal growth factor-like molecule containing mucin-like hormone receptor 1 (EMR-1; *B*), monocyte chemoattractant protein (MCP)-1 (*C*), and CSF-1 (*D*) in kidneys obtained 2 days after ureteral obstruction from mice treated with vehicle or TSA were determined by RT-PCR. Values are means ± SE and were normalized to those for 18S and expressed as relative values of contralateral kidneys obtained from mice treated with vehicle; n = 5. *P < 0.05 vs. values of obstructed kidneys obtained from mice treated with vehicle.

of signals in various physiological and pathophysiological conditions. For example, changes in HDAC2 expression and activities have been shown to mediate neuronal development and memory formation (11, 28). In cardiac muscle, a transient increase in HDAC2 activities contributes to muscle hypertrophy after aortic banding (17). In addition, induction of HDAC4 modulates phenotype changes of skeletal muscle after denervation (34). However, little was known about regulation and function of HDAC in kidney diseases. In the present study, we demonstrate that HDAC1 and HDAC2 are transiently induced in renal tubular cells in the early phase of tubulointerstitial injury caused by UUO. The induction of HDAC1 and HDAC2 likely contributes to the reduced level of histone acetylation and altered gene expression in the tubular cells of the injured kidney. The present study suggests that CSF-1, a chemokine involved in the initiation of tubulointerstitial injury (8, 16, 20), may be regulated by the induction of HDAC1 and HDAC2 in injured tubules. This notion is supported by the observations that a HDAC inhibitor, TSA, attenuated the induction of CSF-1 in vivo and in vitro and that the knockdown of HDAC1 or HDAC2 in tubular cells significantly reduced CSF-1 induction by TNF-α. In addition, valproate, another HDAC inhibitor with a different chemical structure, also reduced CSF-1 induction by TNF-α. These findings suggest that HDAC1 and HDAC2, induced in the renal tubular cells, may modulate proinflammatory responses in the early stage of tubulointerstitial injury.

Indeed, inhibition of HDAC by TSA reduced macrophage infiltration and profibrotic changes after UUO. The inhibition of CSF-1 induction is likely to contribute to a reduction of macrophage infiltration by TSA, since knockdown of CSF-1 has been shown to reduce macrophage infiltration into the interstitium and the subsequent tubular injury (16, 20). In addition to the direct effects of HDAC inhibitor on renal tubular cells, immune-modulating effects of TSA may also play some role in decreased macrophage infiltration since HDAC inhibition has recently been demonstrated to regulate inflammation by modulating immune cells, including dendritic cells (30) and regulatory T cells (35).

A reduction in macrophage infiltration is likely to contribute to the antifibrotic effects of HDAC inhibition in the early stage of UUO. Although a subset of tissue macrophages in the late

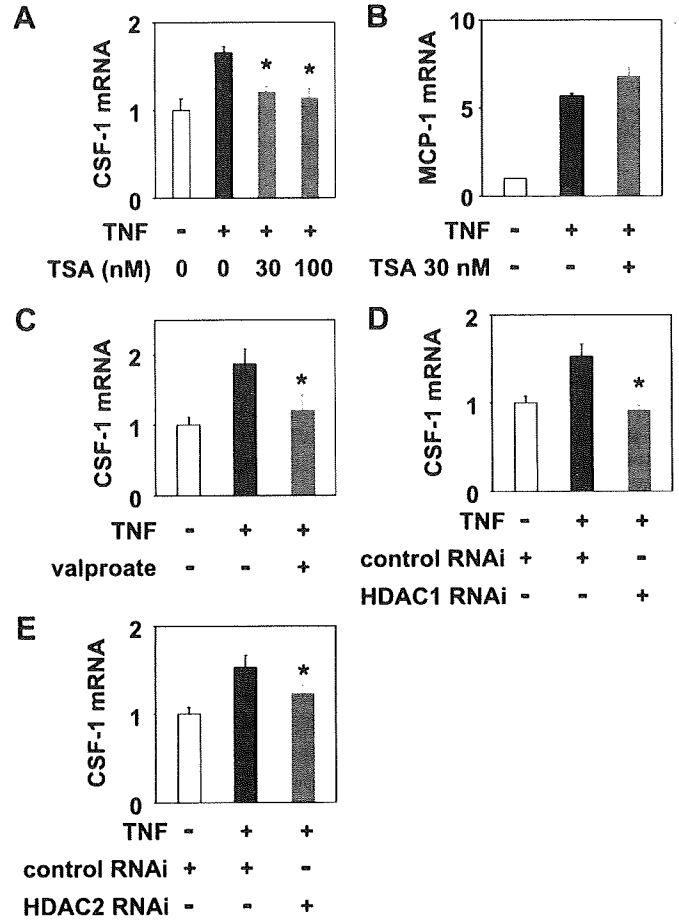

Fig. 7. Knockdown of HDAC1 or HDAC2 attenuates CSF-1 induction in renal tubular cells. *A*: NRK 52E cells were incubated with or without TSA (30 or 100 nM) in the presence of 10 ng/ml TNF-α for 24 h. The level of CSF-1 mRNA was determined by RT-PCR. Values are means ± SE and were normalized to those for 18S and expressed as relative values of control; n = 3–7. *P < 0.05 vs. values with TNF-α alone. *B*: NRK 52E cells were incubated with or without 30 nM TSA in the presence of 30 ng/ml TNF-α for 24 h. The level of MCP-1 mRNA was determined by RT-PCR. Values are means ± SE and were normalized to those for 18S and expressed as relative values of control; n = 8. *P < 0.05 vs. values with TNF-α alone. *C*: NRK 52E cells were incubated with or without sodium valproate (1 mM) in the presence of 30 ng/ml TNF-α for 24 h. The level of CSF-1 mRNA was determined by RT-PCR. Values are means ± SE; n = 7–8. *P < 0.05 vs. values with TNF-α alone. Renal tubular cells were treated with control or HDAC isozyme (HDAC1 in *D* and HDAC2 in *E*) Stealth RNAi (RNA interference) for 24 h. After further incubation with 30 ng/ml TNF-α for 24 h, the mRNA levels of CSF-1 were determined by RT-PCR. Values are means ± SE; n = 8. *P < 0.05 vs. values with TNF-α and control RNAi.

stage of injury mediates resolution of inflammation, the initial phase of macrophage infiltration has been regarded to promote renal fibrosis (1, 2, 8, 19). In addition, the inhibition of epithelial-to-mesenchymal transition by HDAC inhibition (42) may also be involved in reduced fibrosis by TSA to some extent, since a considerable amount of myofibroblasts have been shown to be derived from renal tubular cells by the epithelial-to-mesenchymal transition in UUO-induced fibrotic changes (15).

Although acetylated histones are generally associated with active gene transcription, HDAC inhibition attenuated mRNA levels of CSF-1. The mechanism remains to be elucidated, but we can speculate about some possibilities. For example, HDAC inhibition may lead to an increase in a factor which exerts an inhibitory effect on CSF-1 transcription. It is also possible that HDAC inhibition may reduce recruitment of transcription factors or RNA polymerase II to the CSF-1 promoter, as has been reported for molecules such as c-jun (40) or interferon-stimulated immediate early genes (32).

CSF-1 induction was only partially inhibited by TSA in the present study. However, HDAC activity in nuclear extracts of NRK 52E cells was almost completely inhibited in the presence of 100 nM TSA (data not shown). These results suggest that HDAC may not be the sole activator of the CSF-1 increase under these conditions.

More than 10 HDAC inhibitors have already been examined in clinical trials as antitumor agents with only minor side effects observed (39). In addition to antitumor activities, HDAC inhibitors have been shown to exert beneficial effects on several diseases such as cardiac hypertrophy (4, 18), neuromuscular diseases (3, 10, 25), and inflammatory bowel disease (35). In line with these reports, we and others reported the beneficial effects of HDAC inhibition on glomerular diseases (13, 26). The present study suggests that HDAC inhibitor may also be useful for treatment of tubulointerstitial injury, at least in the early stage. By using the UUO model, the present study clarified that HDAC inhibition reduces tubulointerstitial lesions via a direct mechanism in the tubulointerstitial region independently of glomerular lesions or proteinuria. The precise mechanisms of the renoprotective effects of HDAC inhibitor, especially the target HDAC isozyme, needs to be clarified, considering that different HDAC isozymes can exert even opposite effects under some conditions such as hypertrophy of the heart (4, 36) and angiogenesis (7, 38). In this regard, the present study revealed that HDAC1 and HDAC2, which are increased in injured tubular cells, can act as targets of HDAC inhibitors for reducing CSF-1 expression and inflammation in tubulointerstitial injury.

In conclusion, the present study reveals that HDAC1 and HDAC2 are induced in renal tubular cells in response to tubulointerstitial injury. Increased HDAC1 and HDAC2 in tubular cells are likely to contribute to the expression of CSF-1 and the subsequent inflammatory process. These findings reveal the unrecognized role of HDAC changes in the initiation of tubulointerstitial injury and suggest HDAC inhibition as a potential therapeutic strategy for the treatment of inflammation and fibrosis in the early stage of tubulointerstitial injury.

GRANTS

This work was supported by Mochida Pharmaceutical, Co., Ltd., the Takeda Science Foundation, a Grant-in-Aid for Scientific Research from the Japan Society for the Promotion of Science, and a grant from the Ministry of Health, Labour and Welfare.

DISCLOSURES

No conflicts of interest are declared by the authors.

REFERENCES

1. **Abbate M, Zoja C, Remuzzi G.** How does proteinuria cause progressive renal damage? *J Am Soc Nephrol* 17: 2974–2984, 2006.
2. **Anders HJ, Vielhauer V, Frink M, Linde Y, Cohen CD, Blattner SM, Kretzler M, Strutz F, Mack M, Grone HJ, Onuffer J, Horuk R, Nelson PJ, Schlondorff D.** A chemokine receptor CCR-1 antagonist reduces renal fibrosis after unilateral ureter ligation. *J Clin Invest* 109: 251–259, 2002.
3. **Avila AM, Burnett BG, Taye AA, Gabanella F, Knight MA, Hartenstein P, Cizman Z, Di Prospero NA, Pellizzoni L, Fischbeck KH, Sumner CJ.** Trichostatin A increases SMN expression and survival in a mouse model of spinal muscular atrophy. *J Clin Invest* 117: 659–671, 2007.
4. **Backs J, Olson EN.** Control of cardiac growth by histone acetylation/deacetylation. *Circ Res* 98: 15–24, 2006.
5. **Bascands JL, Schanstra JP.** Obstructive nephropathy: insights from genetically engineered animals. *Kidney Int* 68: 925–937, 2005.
6. **Bokemeyer D, Panek D, Kramer HJ, Lindemann M, Kitahara M, Boor P, Kerjaschki D, Trzaskos JM, Floege J, Ostendorf T.** In vivo identification of the mitogen-activated protein kinase cascade as a central pathogenic pathway in experimental mesangioproliferative glomerulonephritis. *J Am Soc Nephrol* 13: 1473–1480, 2002.
7. **Chang S, Young BD, Li S, Qi X, Richardson JA, Olson EN.** Histone deacetylase 7 maintains vascular integrity by repressing matrix metalloproteinase 10. *Cell* 126: 321–334, 2006.
8. **Eardley KS, Cockwell P.** Macrophages and progressive tubulointerstitial disease. *Kidney Int* 68: 437–455, 2005.
9. **Esteban V, Lorenzo O, Ruperez M, Suzuki Y, Mezzano S, Blanco J, Kretzler M, Sugaya T, Egido J, Ruiz-Ortega M.** Angiotensin II, via AT1 and AT2 receptors and NF-kappaB pathway, regulates the inflammatory response in unilateral ureteral obstruction. *J Am Soc Nephrol* 15: 1514–1529, 2004.
10. **Fischer A, Sananbenesi F, Wang X, Dobbin M, Tsai LH.** Recovery of learning and memory is associated with chromatin remodelling. *Nature* 447: 178–182, 2007.
11. **Guan JS, Haggarty SJ, Giacometti E, Dannenberg JH, Joseph N, Gao J, Nieland TJ, Zhou Y, Wang X, Mazitschek R, Bradner JE, DePinho RA, Jaenisch R, Tsai LH.** HDAC2 negatively regulates memory formation and synaptic plasticity. *Nature* 459: 55–60, 2009.
12. **Haberland M, Montgomery RL, Olson EN.** The many roles of histone deacetylases in development and physiology: implications for disease and therapy. *Nat Rev Genet* 10: 32–42, 2009.
13. **Imai N, Hishikawa K, Marumo T, Hirahashi J, Inowa T, Matsuzaki Y, Okano H, Kitamura T, Salant D, Fujita T.** Inhibition of histone deacetylase activates side population cells in kidney and partially reverses chronic renal injury. *Stem Cells* 25: 2469–2475, 2007.
14. **Ito K, Ito M, Elliott WM, Cosio B, Caramori G, Kon OM, Barczyk A, Hayashi S, Adcock IM, Hogg JC, Barnes PJ.** Decreased histone deacetylase activity in chronic obstructive pulmonary disease. *N Engl J Med* 352: 1967–1976, 2005.
15. **Iwano M, Plieth D, Danoff TM, Xue C, Okada H, Neilson EG.** Evidence that fibroblasts derive from epithelium during tissue fibrosis. *J Clin Invest* 110: 341–350, 2002.
16. **Jang MH, Herber DM, Jiang X, Nandi S, Dai XM, Zeller G, Stanley ER, Kelley VR.** Distinct in vivo roles of colony-stimulating factor-1 isoforms in renal inflammation. *J Immunol* 177: 4055–4063, 2006.
17. **Kee HJ, Eom GH, Joung H, Shin S, Kim JR, Cho YK, Choe N, Sim BW, Jo D, Jeong MH, Kim KK, Seo JS, Kook H.** Activation of histone deacetylase 2 by inducible heat shock protein 70 in cardiac hypertrophy. *Circ Res* 103: 1259–1269, 2008.
18. **Kook H, Lepore JJ, Gitler AD, Lu MM, Wing-Man Yung W, Mackay J, Zhou R, Ferrari V, Gruber P, Epstein JA.** Cardiac hypertrophy and histone deacetylase-dependent transcriptional repression mediated by the atypical homeodomain protein Hop. *J Clin Invest* 112: 863–871, 2003.
19. **Lange-Sperandio B, Trautmann A, Eickelberg O, Jayachandran A, Oberle S, Schmidutz F, Rodenbeck B, Homme M, Horuk R, Schaefer F.** Leukocytes induce epithelial to mesenchymal transition after unilateral ureteral obstruction in neonatal mice. *Am J Pathol* 171: 861–871, 2007.